



Developing a landslide susceptibility map based on remote sensing, fuzzy logic and expert knowledge of the Island of Lefkada, Greece

Paraskevas Tsangaratos¹ · Constantinos Loupasakis¹ · Konstantinos Nikolakopoulos² · Varvara Angelitsa¹ · Ioanna Ilia¹

Received: 27 August 2017 / Accepted: 6 May 2018 / Published online: 14 May 2018
© Springer-Verlag GmbH Germany, part of Springer Nature 2018

Abstract

The main objective of the study was to develop a novel expert-based approach in order to construct a landslide susceptibility map for the Island of Lefkada, Greece. The developed methodology was separated into two actions. The first action involved the construction of a landslide inventory map and the second the exploitation of expert knowledge and the use of fuzzy logic to produce a landslide susceptibility map. Two types of movements were analyzed: rapid moving slides that involve rock falls and rock slides and slow to very slow moving slides. The landslide inventory map was constructed through an evaluation procedure that involved the use of a group of experts, who analyzed data acquired from remote sensing techniques supplemented by landslide records and fieldwork data. During the second action an expert-driven model was developed for identifying the tendency of landslide occurrences concerning both types of movements. A set of casual variables was selected, namely: lithological units, slope angle, slope orientation, distance from tectonic features, distance from hydrographic network and distance from road network. The performance and validation of the developed model were compared with models that are constructed on the bases of each expert's judgment. The results proved that the most accurate and reliable outcomes are obtained from the aggregated values assigned by the group of experts and not from the individual values assigned by each expert. The area under the receiver operating characteristic curves for the models constructed by the expert's group was 0.873 for prediction curves of rapid moving slides and 0.812 for prediction rate curves of slow to very slow moving slides, respectively. These values were much higher than those obtained by each expert. From the outcomes of the study it is clear that the produced landslide susceptibility maps could provide valuable information during landslide risk assessments at the Island of Lefkada.

Keywords Landslide susceptibility · Lefkada · Greece · Fuzzy logic · Persistent scatterer interferometry

Electronic supplementary material The online version of this article (<https://doi.org/10.1007/s12665-018-7548-6>) contains supplementary material, which is available to authorized users.

✉ Paraskevas Tsangaratos
ptsag@metal.ntua.gr

¹ Laboratory of Engineering Geology and Hydrogeology, Department of Geological Sciences, School of Mining and Metallurgical Engineering, National Technical University of Athens, Athens, Greece

² Department of Geological Division of Applied Geology and Geophysics, University of Patras, Patras, Greece

Introduction

Among the Ionian Islands, Lefkada has repeatedly experience strong earthquakes that in most cases triggered secondary damaging and life-threatening phenomena, among which landslides were the most common (Earthquake Planning and Protection Organization 2000; Rondoyanni et al. 2012; Papathanassiou et al. 2013). The geological setting, the steep mountainous relief, the steep slopes that are formed along the coast, the large number of settlements that are developed all around the island and the presence of a dense road network expose Lefkada to a very high landslide risk (Rondoyanni-Tsiambaou 1997). However, estimating the probability of occurrence of a potentially injurious landslide event in a specified time period and in a given area is a highly complex and multi-dimensional problem (Carrara

et al. 1995). On the other hand, the identification of areas susceptible to landslide phenomena, considering only the spatial dimension of the problem could be achieved much easier. Mapping landslide susceptible areas helps in the successful implementation of land-use planning, decision-making and landslide risk reduction strategies.

According to van Westen et al. (1997), landslide susceptibility analysis involves the preparation of a landslide inventory map, the selection and weighting of landslide-related variables and the construction of landslide susceptibility maps. Geomorphological and geological field mapping, visual interpretation of stereoscopic aerial photos, exploitation of very-high-resolution digital elevation models, interpretation and analysis of satellite images including panchromatic, multispectral and synthetic aperture radar (SAR) images are some of the tools used for preparing a landslide inventory map. Particularly, remote sensing has been proven to be a useful tool in landslide hazard and risk assessment, especially in landslide hazard identification, spatial extent prediction and triggering factors detection (Metternicht et al. 2005; Nikolakopoulos 2012; Nikolakopoulos et al. 2015). For rapid moving shallow landslides and debris flows, the hazard identification and inventory mapping can be carried out using optical imageries by recognizing the removal of vegetation from spectral behaviors (Martha et al. 2010), while for slow moving landslides, the mass movement can be detected through image correlations of sequential high-resolution optical data (Casson et al. 2003; Delacourt et al. 2007; Cigna et al. 2013).

Of equal significance is the selection of the appropriate method in order to capture the complex, unknown and non-linear relation between landslide distribution and landslide-related factors (Aleotti and Chowdhury 1999; Lee et al. 2003; Neaupane and Achet 2004; Ayalew and Yamagishi 2005; Pradhan and Lee 2010a; Pourghasemi et al. 2012a; Shahabi et al. 2014). These techniques can be classified into two major categories: qualitative or expert-driven and quantitative or data-driven.

In expert-driven models, there are two types of processes: direct and indirect, in which an expert's judgment plays a significant role. In the direct approach, the expert estimates the boundaries of landslide-prone areas directly in the field, while in the indirect approach experts assign to causal factors weights that represent the influence they have on landslides. Several methods have been used, such as boolean overlay, analytic hierarchy process (Gorsevski et al. 2006; Rozos et al. 2011; Yalcin et al. 2011; Pourghasemi et al. 2012b), fuzzy logic approach (Tangestani 2004, 2009; Champati Ray et al. 2007; Alimohammadlou et al. 2014), multi-class weighting methods (Akgün and Bulut 2007; Rozos et al. 2008; Wang et al. 2009; Kouli et al. 2010, 2014) and spatial multi-criteria analysis (Castellanos and van Westen 2007).

Concerning data-driven models, they use data from past landslides in order to obtain information on the relative importance of each factor on a statistical or probabilistic base. There are three main approaches: bivariate statistical analysis that includes a likelihood ratio model (Lee 2004; Pourghasemi et al. 2014; Youssef et al. 2015a); the information value method (Yin and Yan 1988; Sarkar et al. 2013) and the weight of evidence modeling (Pourghasemi et al. 2012c; Kouli et al. 2014; Neuhauser et al. 2012; Ilia and Tsangaratos 2016; Torizin 2016). Multivariate methods that include logistic regression and discriminant analysis (Dai and Lee 2003; Guzzetti et al. 2005; Frattini et al. 2008; Sabatakakis et al. 2013; Youssef 2015). Data mining techniques include fuzzy logic (Ercanoglu and Gokceoglu 2004; Pourghasemi et al. 2012c; Tien Bui et al. 2012a; Yiping et al. 2014), decision tree models (Nefeslioglu et al. 2010; Yeon et al. 2010; Tien Bui et al. 2012b; Pradhan 2013; Youssef et al. 2015b; Tsangaratos and Ilia 2016), artificial neural networks (Ermini et al. 2005; Caniani et al. 2008; Melchiorre et al. 2008; Li et al. 2014; Tsangaratos and Benardos 2014), support vector machine (Yao et al. 2008; Yilmaz 2010; Marjanovic et al. 2011; Xu et al. 2012; Tien Bui et al. 2012b; Pourghasemi et al. 2013; Hong et al. 2015), and neuro-fuzzy (Pradhan et al. 2010; Vahidnia et al. 2010; Sezer et al. 2011; Oh and Pradhan 2011; Tien Bui et al. 2012c).

Comparing the models of the two categories, the expert-based models appear subjective and often ignore the fuzziness of expert judgment. In addition, the accuracy of the results depends significantly on the experience and time involvement of the expert. However, expert-based models may provide highly accurate results as they appear to be an efficient approach for landslide phenomena that are caused by different mechanisms (Ruff and Czurda 2008). Data-driven models are influenced by the availability and the quality of data, with data of poor quality producing less accurate predictive models. It is also known that bivariate statistical analysis and multivariate methods work well only if certain statistical criteria are satisfied, while data mining methods produce complex and often hard to interpret models. Despite their different approach most of these techniques share a common process. They involve the analytical examination of the settings of known landslide-prone areas, in order to provide information and knowledge regarding possible future landslides (Varnes 1984; Guzzetti et al. 1999; Aleotti and Chowdhury 1999; Fell et al. 2008).

In this context, the main objective of the present study was to develop a two-action evaluation procedure for constructing a landslide inventory map and a landslide susceptibility map for the Island of Lefkada. The construction of the inventory map was based on the work of a group of experts, which analyzed data acquired from remote sensing techniques complemented by landslide records and field data. Two types of movements were analyzed: rapid moving

slides that involve rock falls and rock slides and slow to very slow moving slides. The construction of the landslide susceptibility map was achieved by applying methods that are based on the concept of fuzzy logic and expert knowledge. The computation process was carried out using Microsoft Visual Studio 2010 for the estimation of the weights of each landslide-related variable and ArcGIS 10.1 (ESRI 2011) for the analysis of the data and the production of the landslide susceptibility maps.

The study area: general settings

The Island of Lefkada covers about 335 km² with 117 km of coastline (Fig. 1a). Approximately, 70% of the area is characterized as mountainous, with the highest peak, Stavrota (1182 m), located in the central part of the island. The west side of the island exhibits a very steep morphology and also abrupt deepening of the seabed. The coastline is occupied by sandy beaches and steep slopes. The east side of the island is covered by large flat areas, while the seabed is shallow with many islets. Inland there are narrow plateaus, fertile valleys, and deep ravines with intense vegetation. Over 30% of the area is covered by agriculture and natural vegetation, 25% covered by sclerophyllous vegetation, 12% by olive

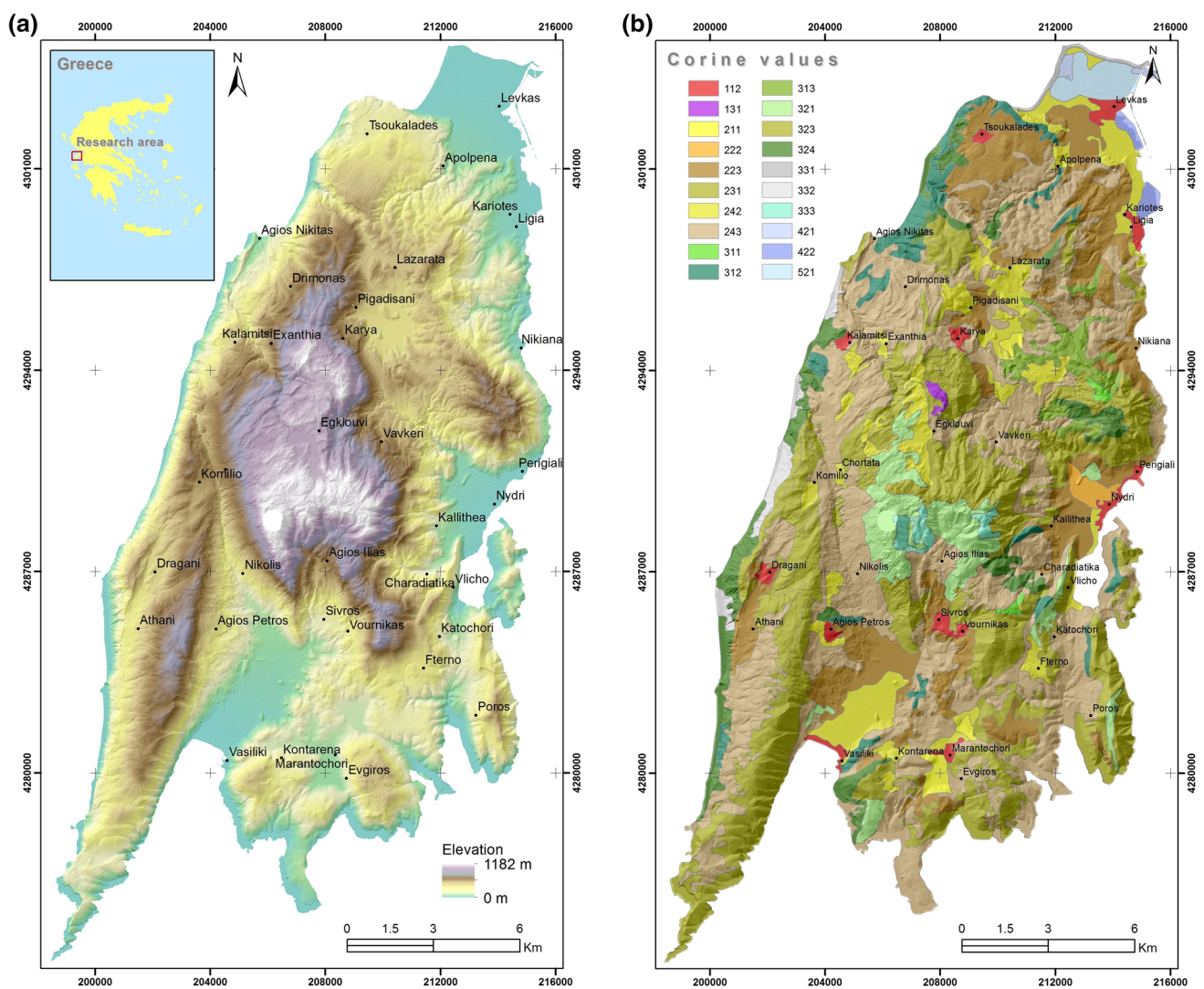


Fig. 1 a The study area, b the Corine Cover. Corine legend: 111 continuous urban fabric, 131 mineral extraction sites, 211 arable land, 222 fruit trees and berry plantations, 223 olive groves, 231 pastures, 242 complex cultivation patterns, 243 agriculture and natural vegeta-

tion, 311 broad-leaved forest, 312 coniferous forest, 313 mixed forest, 321 natural grassland, 323 Sclerophyllous vegetation, 324 transitional woodland-scrub, 331 beaches, dunes, sands, 332 bare rocks, 421 salt marshes, 422 salines, 521 coastal lagoons

groves and 7% by complex cultivation patterns (Fig. 1b). The climate of Lefkada is characterized as Mediterranean, with mild summers and mild and very wet winters. The average monthly temperatures range from 9.9 °C (January) to 25.3 °C (August). The average annual rainfall (data from the Lefkada meteorological station, 38°37'N, 20°43'E for the period 1975–1997, 22 years) reaches up to 916.8 mm and the average monthly rainfall range from 9.5 mm (June) to 198.6 mm (November). From a new meteorological station (38°49'50"N, 20°42' 42"E) operating since August 2009 (8 years), the average annual rainfall reaches up to 1200 mm.

Geological and tectonic settings

The largest part of Lefkada, mainly the eastern part, belongs to the Ionian geotectonic zone, while its western part belongs to the Paxos zone. The Paxos zone consists of evaporites and limestone formations, covered by Neogene clastic sediments, mainly marls and Miocene sandstones. The Ionian zone includes Paleocene limestones, dolomitic limestones and siliceous schist partly covered by flysch formations of Oligocene–Middle Miocene age. The Neogene sediments consist of conglomerates, sandstones, marls and marly limestones. Opposed to the other Ionian Islands, the Quaternary sediments found at Lefkada outcrop to a very limited extent, while the Pleistocene marine and lacustrine deposits present a larger extent (Rondoyanni et al. 2012) (Fig. 2a). Based on their geotechnical behavior, the outcropping formations can be grouped as (Fig. 2b) (Bornovas 1964; Rondoyanni-Tsiambaou 1997): (a) recent alluvial deposits of various lithological compositions, consisting mainly of clays, sandy silts, sands, pebbles, cobbles and nibbles of various grain size dimensions; (b) scree and talus cones, which are composed of unconsolidated sediments of cobbles, rubbles, sands and sandy clays, found along the mountain slopes and torrent outlets; (c) flyschoid sediments, which are characterized as clastic sediments, mainly consisting of blue marls, sandstones, sandy clays, siltstones and thin micro-brecciated limestones; (d) limestones with flat-pebble conglomerates; (e) massive limestone formations; (f) dolomite formations and (g) schist formations.

Lefkada's high seismicity, with earthquake surface-wave magnitudes values (M_s) ranging between 6.1 and 7.2, is attributed to the fact that the island holds a key position along the 140 km-long Cephalonia Transform Fault (CTF), where the Hellenic subduction in the South passes to the Adriatic collision in the North (Papazachos and Papazachou 1989; Louvari et al. 1999; Sachpazi et al. 2000; Papadopoulos et al. 2003; Kokinou et al. 2006). GPS data indicate onshore shortening at a rate of 2–3 mm/year with velocity values decreasing from north to south (Ganas et al. 2012). Several active and neotectonic faults, striking N–S and NE–SW, were also located on

South Lefkada (Fig. 2a), the most important of which can be considered the Athani fault (Lekkas et al. 2001; Rondoyanni et al. 2012).

Landslide movement types in Lefkada Island

Landslide movements were classified according to the Cruden and Varnes Classification (1996) as rock falls and rock slides and as rotational or translational slides. Rock fall is considered as a landslide that involves the collapse of a mass material from a steep slope, whereas a slide is considered as a down-slope movement of a mass material that occurs along a distinctive surface. If the surface is curved the slide is referred to as rotational while if the surface is straight then it is referred to as translational or planar (Cruden and Varnes 1996). Most of them were located near the island's road network and coast line (Fig. 3). Extended slope failures of all aforementioned categories were observed in areas covered by thick-bedded limestone formations that form steep slopes and at the toes of those slopes when extensive cones of scree materials are present. In addition it should be noticed that the presence of thin marly horizons within the limestone formation increases the likelihood of landslides.

Regarding the triggering mechanism, seismicity and rainfalls are the two main triggering factors. Considering the study area, Rondoyanni et al. (2012) reported that rock falls and other landslides, as well as liquefaction phenomena and small-scale subsidence, are the main secondary effects due to earthquakes. The intensity of landslide events during earthquakes is also presented by Papathanassiou et al. (2013). The authors produced a landslide inventory map after the 2003 earthquake event (moment magnitude value $M_w = 6.3$) integrating pre and post seismic satellite imagery as well as reports from field surveys. Similar effects had been observed after the November 2015 earthquake event ($M_w = 6.4$) that caused two casualties and numerous reported damages in buildings and road network. This earthquake caused a significant amount of rock falls and rock mass slides reported mainly Egremni and Port Katsiki beaches (Fig. 4a–c) in Dragani villages (Fig. 4d) and the road connecting the villages of Tsoukalades and Agios Nikitas (Fig. 4e) (Ganas et al. 2015). Concerning the triggering effect of rainfall, limited records were available for the research area. However, based on former experience intense rainfall was responsible for the manifestation of the majority of the reported rotational and translational slides (Koukis and Ziourkas 1991; Koukis et al. 2005).

Data and methods

The developed susceptibility mapping methodology was based on a fuzzy additive weighting model that captures the knowledge of a group of experts and tackles uncertainty

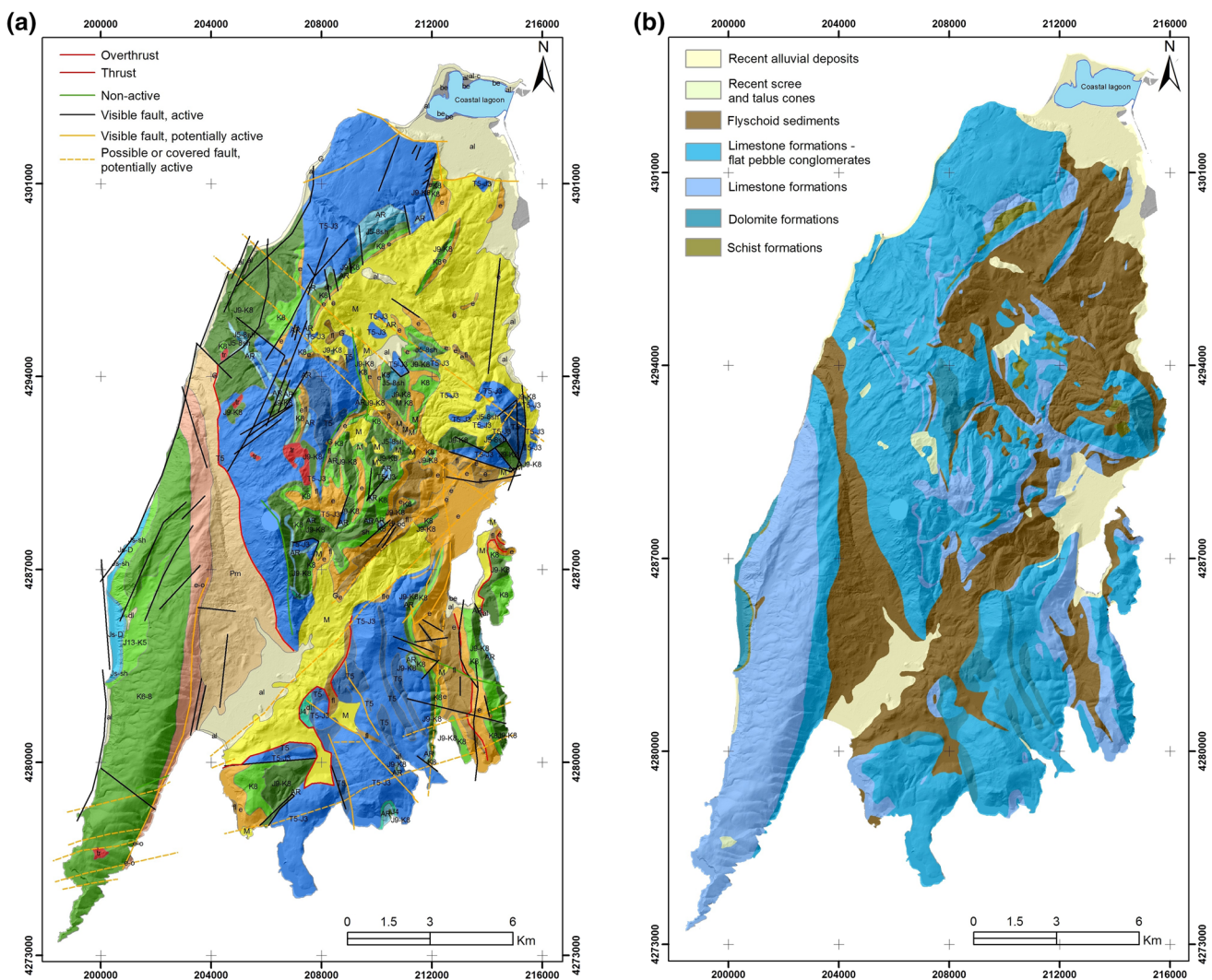


Fig. 2 **a** Geologic map of Lefkada Island (modified from IGME 1963); al: Holocene alluvial deposits, al–c: Holocene recent scree and talus cones, be: Holocene marsh deposits, tr: Holocene Terra rossa, dl: Pleistocene scree and old talus cones, dl–c: Pleistocene cohesive scree, Pm: Miocene marls, Paxos Zone: e–o: Paleocene limestones, K6–8: Upper Cretaceous limestones, J13–K5: Lower Cretaceous limestones, Js–D: Upper Jurassic limestones, Js–sh: Upper Jurassic

schists, Ionian Zone: M: Miocene molassic, G: Miocene evaporites, fl: Upper Eocene flysch, e: Paleogene limestones, K8: Upper Senonian limestones, J9–K8: Upper Jurassic–Lower Senonian limestones, AR: Lower Jurassic Ammonitico Rosso, limestones, J5–8sh: Lower Jurassic schist formations, J4: Domerian limestones, T5–J3: Upper Triassic limestones, T5: Lower Norian Dolomite; **b** unified geological formations map

and imprecision by representing experts’ judgment as fuzzy numbers. This is the main difference from previous studies that utilized expert’s knowledge. Uncertainty and subjectivity that may follow the implementation of expert knowledge is handled through fuzzy logic. For the methodology implementation, the authors of this study played the role of experts due to their professional expertise in the fields of natural hazards, engineering geology and remote sensing. In this context, one expert played the role of coordinator. The developed methodology was separated into two main actions: the first action involved the construction of the landslide inventory map and the second the application of fuzzy logic approach to produce a landslide susceptibility map.

Figure 5 illustrates in detail the flowchart of the developed methodology.

Construction of the landslide inventory map

The first action of the developed methodology was the production of the landslide inventory map from the group of experts. Rapid movements were identified by conventional techniques that involved the examination of satellite images and aerial photos that were included in previous studies (Rondoyanni-Tsiambaou 1997; Lekkas et al. 2001; Papadopoulos et al. 2003; Papathanassiou et al.

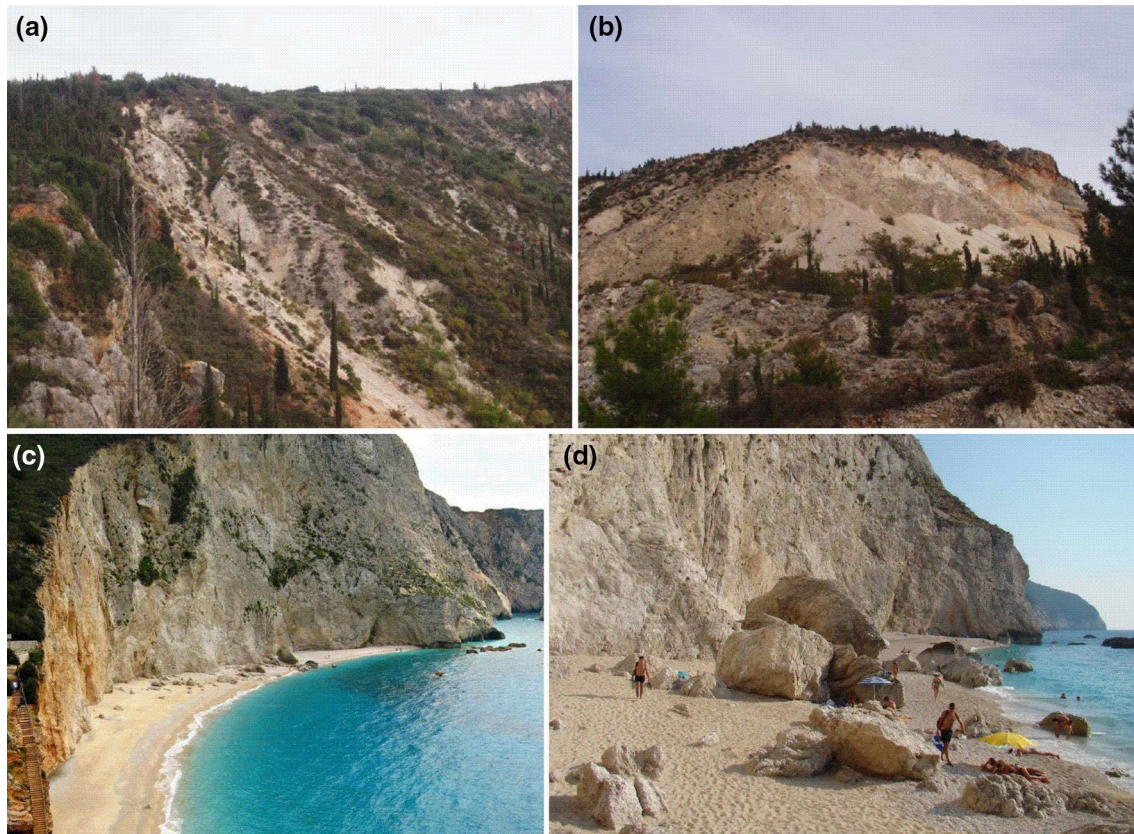


Fig. 3 **a** Extended complex failure (rock slides and rock falls) in thin bedded limestone, W of Kalamitsi Village; **b** rock falls along a thrust and creep movements at the scree materials, thin bedded limestone,

SW of Kalamitsi Village; **c, d** over-sized rock falls at the Porto Katsiki beach, conglomerate limestone, northern end of the west coast-line of the island

2005, 2013; Rondoyanni et al. 2012) and extensive field-work (during the summer of 2014), while for slow to very slow movements DinSAR images, processed by applying the persistent scatterers interferometry (PSI) technique, were used (Fig. 6a, b). Concerning the slow to very slow movements, in the scientific literature several studies that analyze PSI data (highly reflective point-wise targets, the so-called permanent scatterers, PSs) combining the results with conventional geomorphological approaches, such as aerial photo-interpretation coupled with pre-existing landslide inventory maps can be found (Colesanti and Wasowski 2006; Greif and Vlcko 2012; Raspini et al. 2013, 2014; Tofani et al. 2013). In the current study, three data sets of PSI data (one ascending, ERS data acquired in 5/11/1995–12/7/1999, and two descending, ERS and ENVISAT data, acquired in 19/4/1992–18/1/2000 and 25/6/2003–23/6/2010, respectively) were provided by Tele-Rilevamento Europa. The PSI data were processed within the framework of the TerraFirma project, supported by the Global Monitoring for Environment and Security Service Element Program, promoted and financed by European Space Agency. PSI data processing involved the

analyses of the standard deviation values, σ , of the average rate of deformation and the identification of the ground displacements trend (Sakkas et al. 2014). PSs points exhibiting high σ values were excluded from the data set, while PSs declining intensities from the surrounding points were initially identified as ground surfaces affected by sliding movements.

The next phase during the first action was to produce a map illustrating the kernel density of the PSs. The map allowed the group of experts to point out sites where slow to very slow movements is evident. Kernel Density, an Arc-Map 10.1 function included in the Spatial Analyst Toolbox, was used to calculate the density per unit area of PSs using a quadratic kernel function to fit a smoothly tapered surface to each PSs dataset.

Finally, each expert constructed a landslide inventory map concerning the inventoried number and type of the landslides. These maps were later presented to the coordinator. The coordinator compared the results and returned a new aggregated landslide inventory map to each expert for verification. If the aggregated landslide inventory map was approved, the landslide inventory map was finalized. If

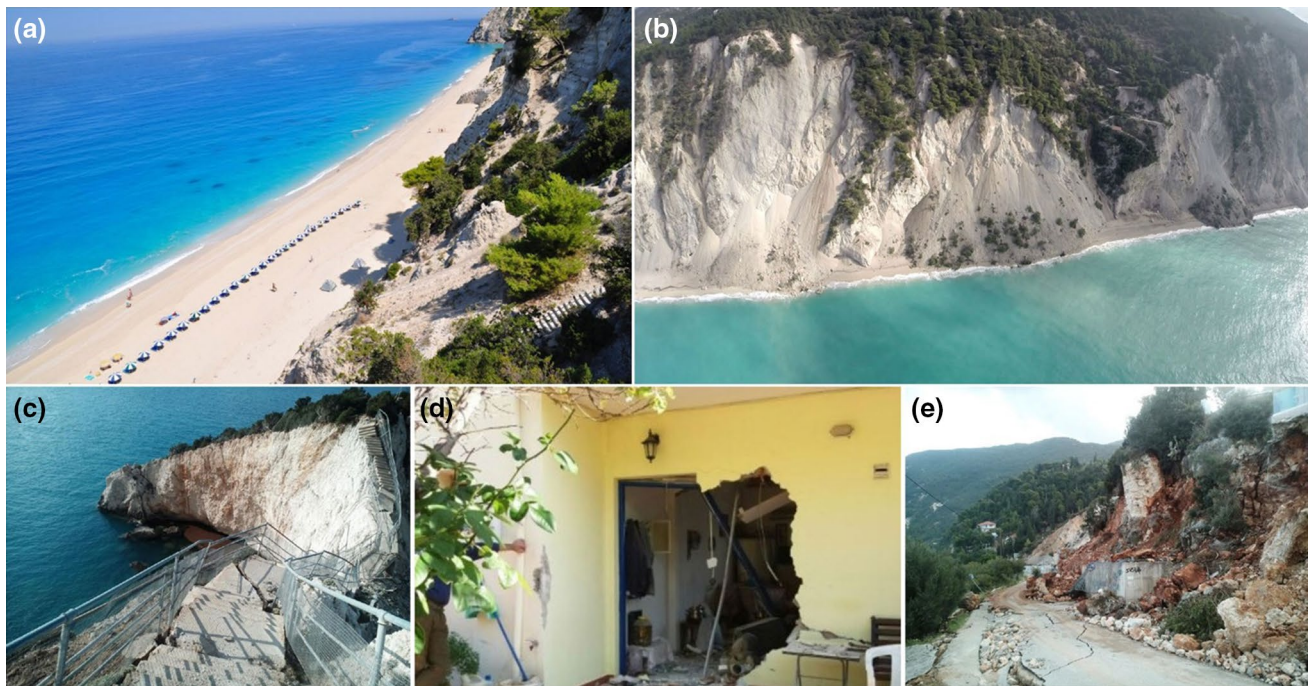


Fig. 4 Egremni beach before (a) and after (b) the 2015 earthquake. The beach was practically buried under the scree materials; c damaged path to Porto Katsiki cape (Ganas et al. 2015); d over-sized rock

fall entering a house. It caused the death of a 65-year-old woman; e rotational slide along the road connecting Agios Nikitas with Tsoukalades (Ganas et al. 2015)

not, a second attempt was given (Fig. 5). The process was stopped when all experts agreed on the type and number of landslide events.

Construction of the landslide susceptibility map

Taking into account the objectives of the study, the availability of the existing resources and data, the extension and complexity of the area and also the types of landslides the variables used for the landslide susceptibility assessment were selected. Specifically, lithology, slope angle, slope orientation, distance from tectonic features, distance from hydrographic network, and distance from road network were among the six variables that were selected for analysis.

Lithology is one of the most important factors, controlling ground movements, both rapid and slow (Koukis et al. 2005). The group of experts, based on field observations as well as on their former experience assessed the weights of the different formations towards rock fall (rapid) and slide (slow) failures susceptibility. The orientation along with the angle of slopes plays a very important role in the concept of landslide manifestation as causative factors. This is because they are expressing the result of the combined influence of many parameters, such as the intensity of climatic conditions, the weathering processes, the types and density of

vegetation and the discontinuity pattern (internal geometry) of geological formations (Huma and Radulescu 1978; Carrara 1983). Also, slope angle directly affects on shear stress and indirectly controls surface water velocity (degree of saturation). The degree of saturation of slope forming material has significant control over the occurrence of landslides. Previous studies have shown that landslides are usually abundant on N, NNE and SSW orientated slopes, a fact that was attributed mainly to climatic factors (Koukis and Ziourkas 1991). In Greece, the SE–SW (135° – 225°) oriented slopes are affected the most by rainfalls, due to the counterclockwise circulation of the clouds, and the NNW–NNE (315° – 45°) oriented slopes are the most sunless. The increase of the slope steepness and the loss of support along the base of the slopes that is mainly observed during the construction of roads may reduce the safety factor and increase the possibility of a landslide if mitigation measures are absent. Faults are the structural features generating a zone of weakness, along which landslide susceptibility is highest. It has generally been observed that the probability of landslide occurrence increases for areas close to faults, which not only affect the morphology and the terrain permeability, but also contribute to the rock mass fragmentation and erosion generating a zone of weakness (Kouli et al. 2010). Several studies have proven that proximity to river networks is an important factor controlling the occurrence of slides (Gokceoglu and Aksoy 1996). This can be attributed

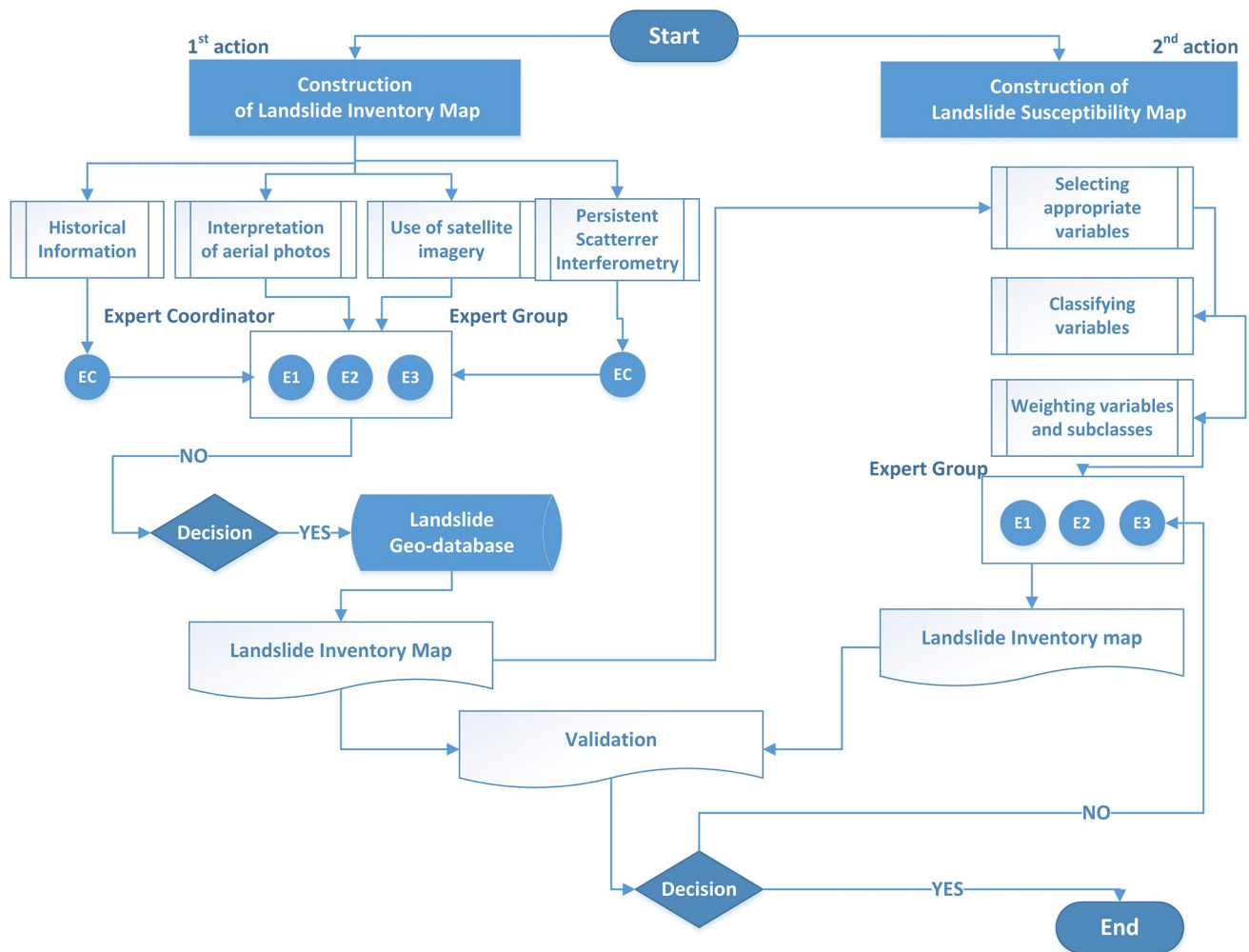


Fig. 5 Flowchart of the developed methodology

to the fact that morphological alterations caused by gully erosion may influence the initiation of landslides and also that maximum infiltration is generally observed on slopes that are near river networks. This process is further induced when the slopes of certain geological formations present increased permeability. Some of the necessary data sets were directly digitized from the original thematic maps (eg: geological maps) while others were derived from spatial GIS calculations.

The most essential stage of the implementation is the process of dividing each input, into classes. This task was performed by the coordinator. Expert knowledge and statistical analysis can be useful means for defining the classes. Lithology was classified into seven categories based on the geotechnical behavior of the outcropping formations, as previously described (Fig. 2b). Slope angle was classified into five classes ($<15^\circ$, $16^\circ\text{--}30^\circ$, $31^\circ\text{--}45^\circ$, $46^\circ\text{--}60^\circ$ and $>61^\circ$) (Fig. 7a) and slope orientation into eight classes ($0^\circ\text{--}45^\circ$, $46^\circ\text{--}90^\circ$, $91^\circ\text{--}135^\circ$, $136^\circ\text{--}180^\circ$, $181^\circ\text{--}225^\circ$, $226^\circ\text{--}270^\circ$, $271^\circ\text{--}315^\circ$,

$316^\circ\text{--}360^\circ$) (Fig. 7b). Concerning the tectonic structures influence, multiple buffer zones (<100 , $101\text{--}500$ and >501 m) were generated around the fault lineaments taking into account the type (normal, uplift) and the activity (active, inactive) of the faults (Fig. 8a). A drainage buffer map was produced based on stream order and streams were buffered at a distances of <50 , $51\text{--}100$ and >101 m (Fig. 8b). Finally, a buffer zone of 50 m to either side of dirt roads was applied, producing two classes, while similarly, multiple buffer zones were applied to paved roads producing three classes (within a distance of 50, $51\text{--}100$ and >101 m) (Fig. 9). The calculation of the weights of the classified variables was conducted by applying a fuzzy logic approach, which is described in detail at the following paragraph.

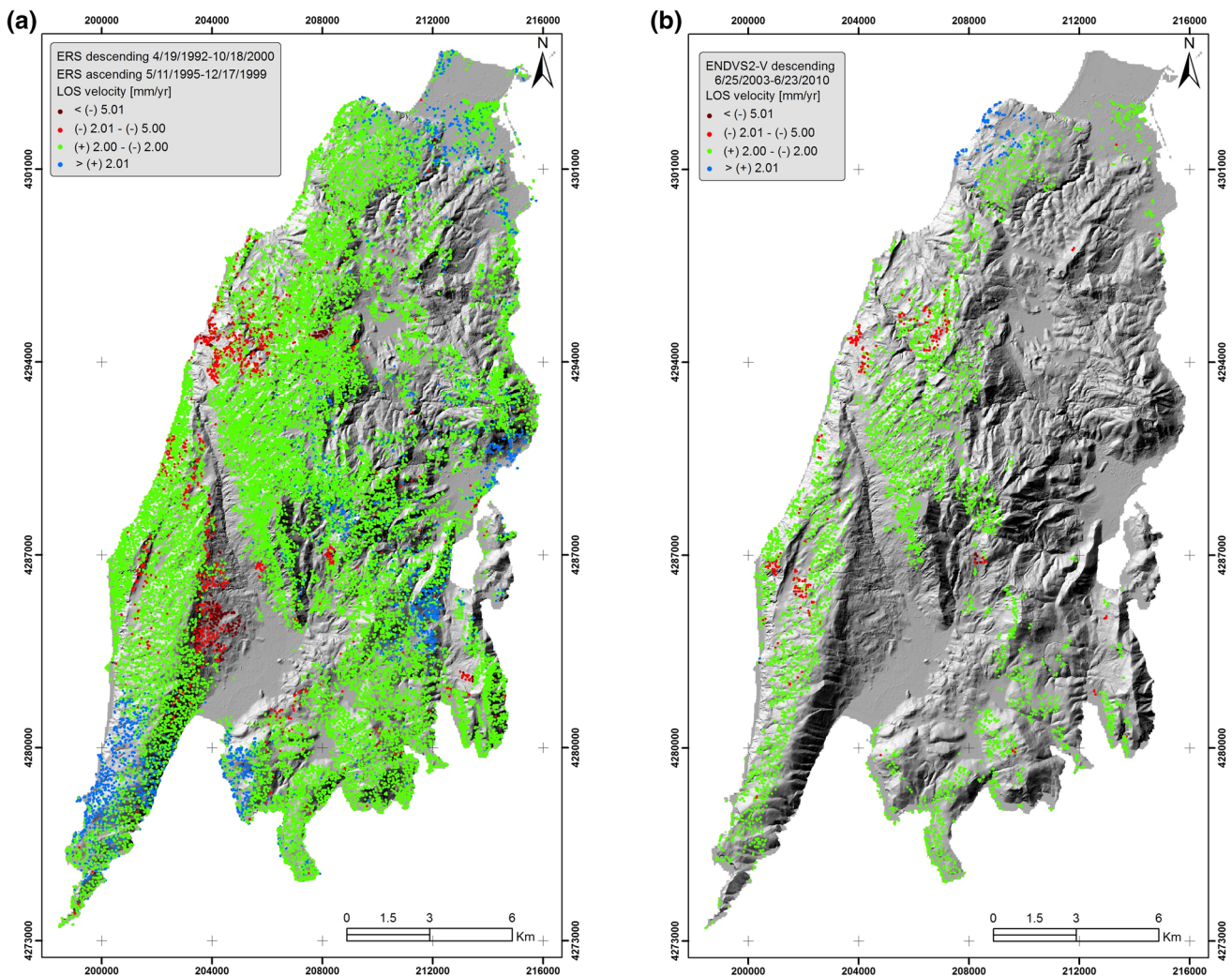


Fig. 6 a Classified PSI data sets from the ascending and descending orbits of ERS1/2, b descending orbits of ENVISAT

Application of a fuzzy logic approach for weighting the variables

The present weighting procedure utilizes a group of experts that use a fuzzy simple additive weighting model in order to weight each subclass as well as the main landslide-related variables (Chou et al. 2008; Kabassi 2009). A set of linguistic variables was used for approximate reasoning and to represent the original domain set, while the weights of the five-level fundamental scales of importance were expressed via the trapezoidal fuzzy numbers (Zadeh 1965; Kaufmann and Gupta 1991; Zimmermann 2001) (Table 1).

The fuzzy simple additive weighting techniques based on the above conceptual model was applied as follows (Chou et al. 2008):

Step A Establishment of the group of experts, and selection of the variables that better express the Landslide Susceptibility Index.

Step B Determination of the reliability of each expert. The comparative importance of each individual expert must be considered to enhance the performance. If all the experts are considered at same expertise level, the group is thought as homogenous otherwise the group is called heterogeneous. The degree of reliability, dR_t , is based on the values presented in Table 2, where $dR_t \in [0,1]$ and $t = 1, 2, \dots, k$, the number of experts.

The final reliability weight of each expert is calculated by the equation:

$$wdR_t = \frac{dR_t}{\sum_{t=1}^k dR_t}, \tag{1}$$

$t = 1, 2, \dots, k$ the number of experts.

Step C Introduction of the linguistic weighting variable for each expert (taking into account his reliability wdR_t)

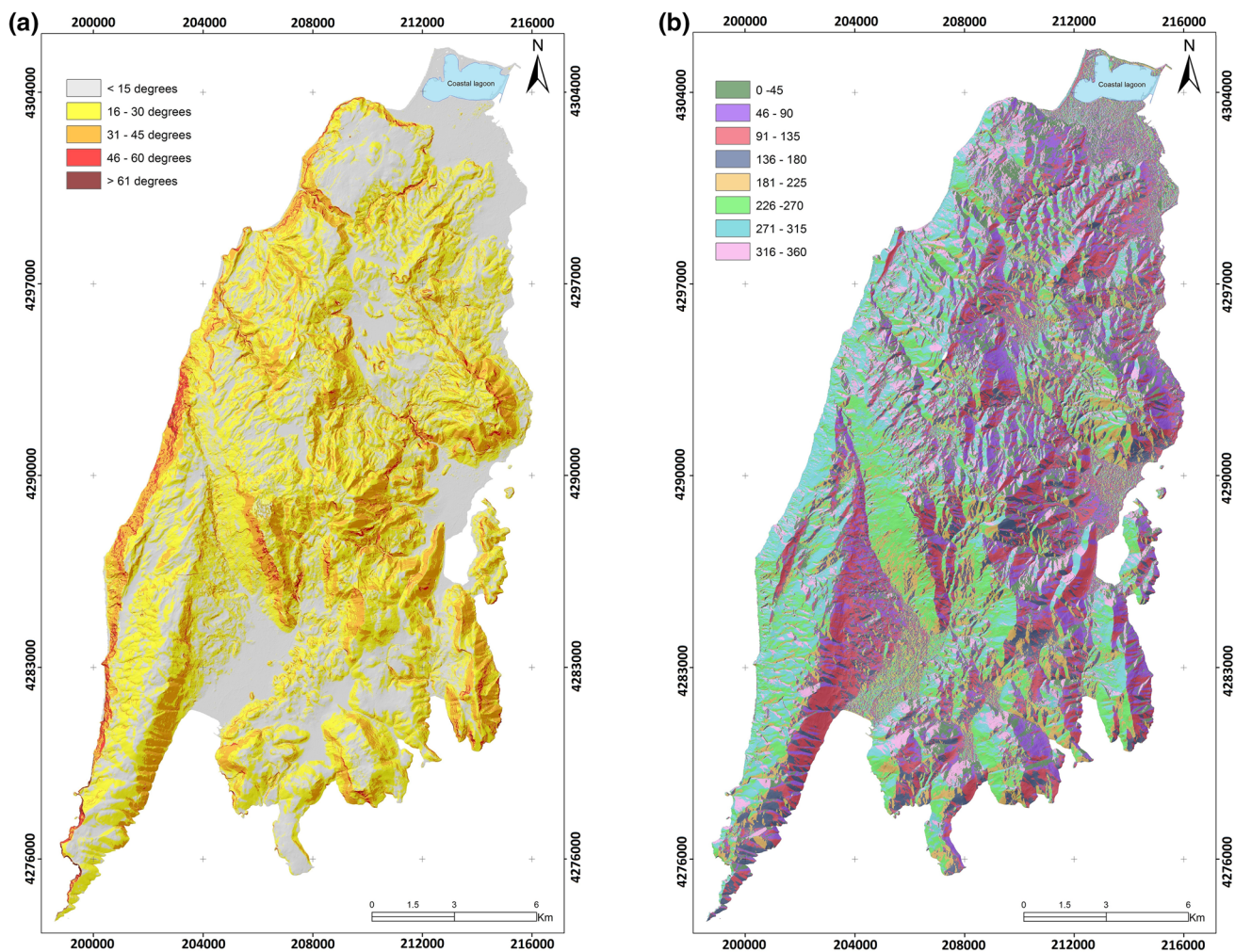


Fig. 7 Landslide conditioning factors: **a** slope angle; **b** slope orientation

in order to assess a variable’s importance and compute the aggregated fuzzy weights of individual variables (Table 1).

The calculation of the aggregated fuzzy variable weight was conducted as follows:

The $\tilde{W}_{jt} = (a_{jt}, b_{jt}, c_{jt}, d_{jt})$ is the fuzzy number of the j th variable expressed by the t th expert. The aggregated fuzzy variable weight for the j th variable is defined as $\tilde{W}_j = (a_j, b_j, c_j, d_j)$, where $a_j = \left(\sum_{t=1}^{k0} wdR_t \times a_{jt} \right)$, $b_j = \left(\sum_{t=1}^{k0} wdR_t \times b_{jt} \right)$, $c_j = \left(\sum_{t=1}^{k0} wdR_t \times c_{jt} \right)$, $d_j = \left(\sum_{t=1}^{k0} wdR_t \times d_{jt} \right)$.

Step D Defuzzification the weights of individual variables, according to the centroid method and compute the normalized weights. The normalized weights are assigned to each variable through certain spatial functions producing the appropriate weighted raster files.

Landslide susceptibility mapping

The construction of the landslide susceptibility map was achieved by combining all the weighted variables according to Eq. (2) and the usage of Raster Calculator. Raster Calculator is a geoprocessing tool for performing raster analysis using a Map Algebra expression and is found within the Spatial Analyst Toolbox (ESRI 2011):

$$Ls_i = \frac{1}{n} \left(\sum_{i=1}^n \sum_{j=1}^k w_{ij} x W_i \right), \tag{2}$$

where n is the number of the landslide-related variables, w_{ij} the weight factors of the j th class of the i th variable and W_i the overall weight of the i th variable, respectively. The higher the membership value, the more susceptible is the

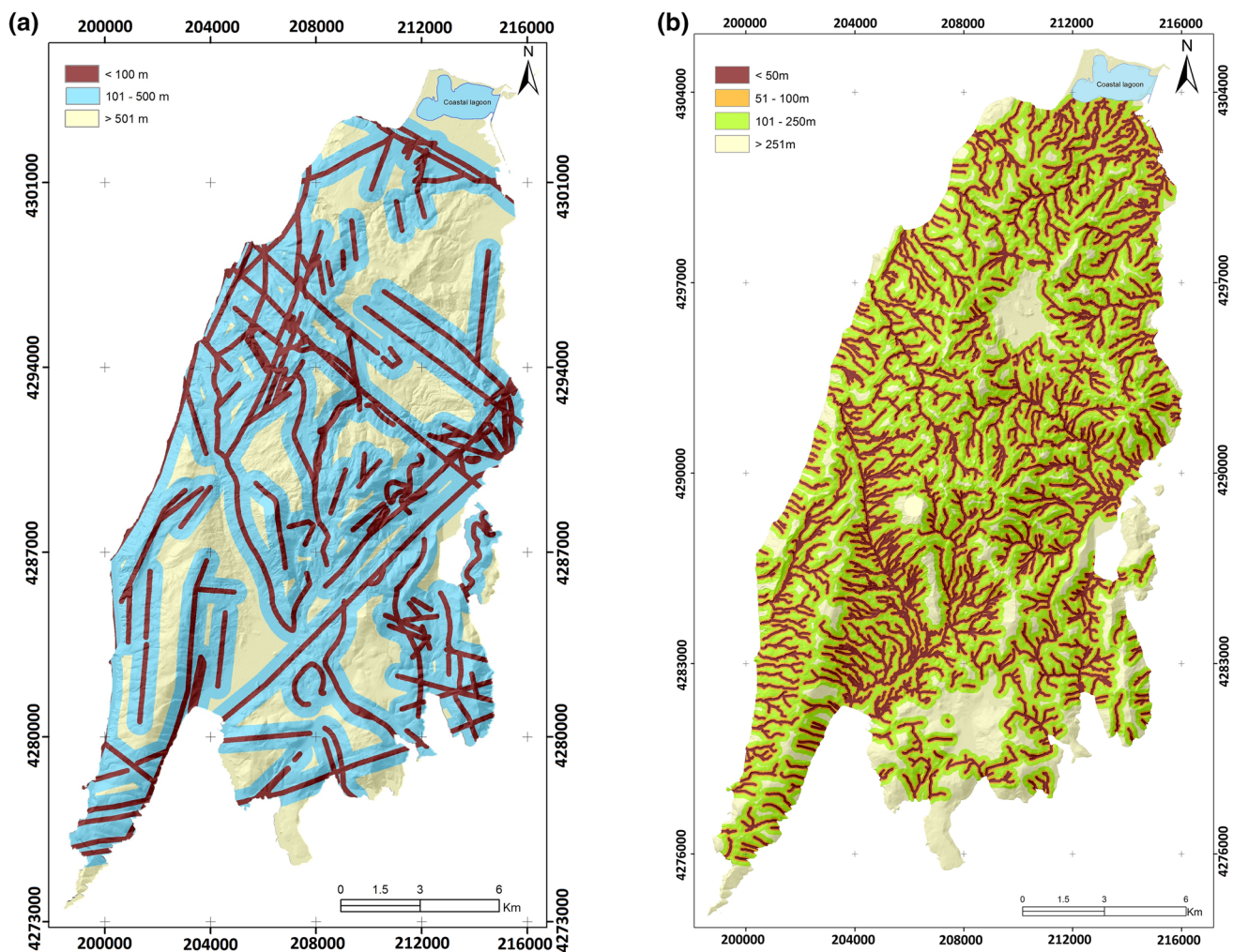


Fig. 8 Landslide conditioning factors: **a** distance to tectonic features; **b** distance to hydrographic network

terrain unit to the occurrence of landslides and vice versa. The landslide susceptibility map was classified into five categories of susceptibility, namely very high susceptibility (VHS), high susceptibility (HS), moderate susceptibility (MS), low susceptibility (LS) and very low susceptibility (VLS), using the natural break method for the determination of the class intervals (Feizizadeh and Blaschke 2013).

Validation of the landslide susceptibility map

The final phase was the validation phase. According to Guzzetti et al. (2005, 2012), landslide susceptibility assessments are spatial predictive models and should be evaluated against the information used to prepare the prediction. Pradhan and Lee (2010b) considered a reliable validation metric, increasing the landslide density ratio when moving from low susceptible classes towards high susceptible classes. The

validation process was performed by comparing the produced landslide susceptibility map with the actual landslide locations using prediction rate methods (Chung and Fabbri 2003). For each susceptibility map the calculated area under curve (AUC) helped in estimating the predictive power of the model (Pham et al. 2015, 2016). It should be mentioned that all evaluations and comparisons concerning AUC values were based on a traditional academic point system (Bozikov and Zaletel-Kragelj 2010).

Results

During the first action, the construction of the landslide inventory map and specifically the phase of analyzing the PSI data, three datasets (one ascending ERS dataset, and two descending, ERS and ENVISAT datasets) were evaluated. Based on the methodology, PSs that exhibit high σ values were excluded from the data set, since they were considered

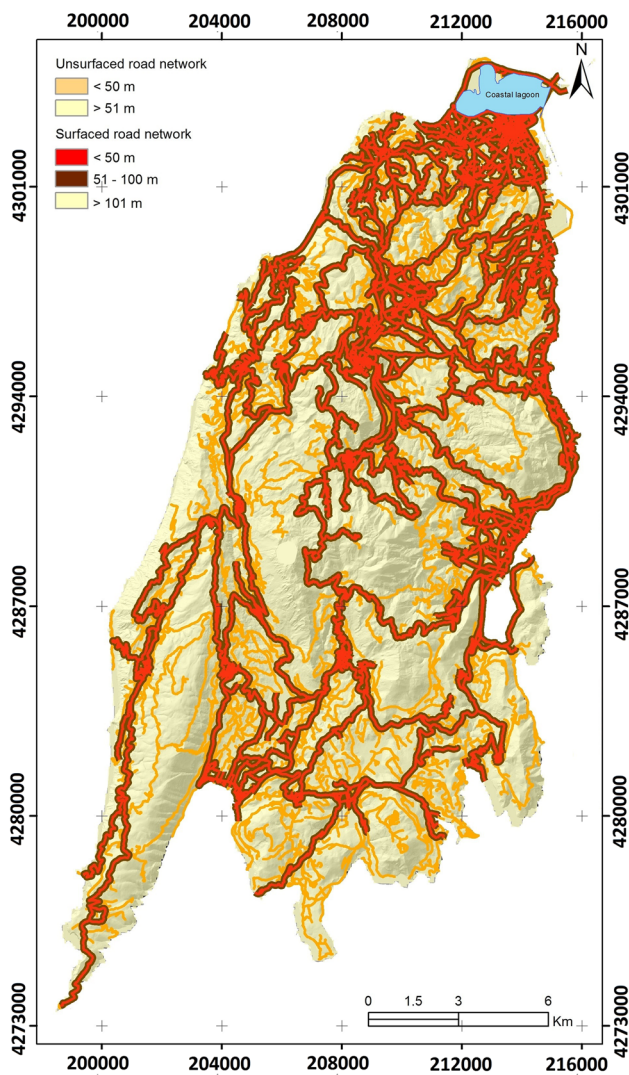


Fig. 9 Landslide conditioning factors: distance to road network

Table 1 Linguistic variables, crisp and fuzzy numbers for the importance weight

Linguistic variables	Crisp numbers	Fuzzy numbers
Very low importance	1	(0, 0, 0, 3)
Low importance	2	(0, 3, 3, 5)
Medium importance	3	(3, 5, 5, 7)
High importance	4	(5, 7, 7, 10)
Very high importance	5	(7, 10, 10, 10)

as defective points affected by morphologic or atmospheric induced noise. For the ERS data sets, it came out that the PSs velocities present a rather uniform pattern all over the island with small values ranging from 0.11 up to 0.98 mm/year, for the descending data set and from 0.14 up to 1.40 mm/year for the ascending 1. A similar pattern was identified for the

Table 2 Degree of expert’s reliability

Linguistic variables	Degree of experts reliability (dR)
Low reliability	0.50
Medium reliability	0.75
High reliability	1.00

descending ENVISAT data, with values ranging from 0.13 to 1.58 mm/year. According to the methodology, this indicates that all available data could be accepted for further analysis. The next phase was to estimate the linear trend of each PS by applying kernel density function and to select those that present intensive variability of the displacement rate, with respect to the surrounding PSs, pointing to slow landslide movements. The selected data set consisted of 1745 PSs with displacement rates varying from -23.0 to -2.0 mm/year. Figure 10a illustrates the kernel density map of these points, indicating the areas with sliding displacements with respect to the surrounding points. Finally, after the evaluation of the above described data, the landslide inventory map approved by the experts, for both types of landslides, is presented in Fig. 10b. A total number of 174 movements were identified, with 45 classified as slow to very slow movements and the remaining 129 as rapid movements.

As proposed by the developed methodology, during the second action, a group of three equally reliable ($dR = 1$) experts assigned to each landslide-related variable (Tables 3, 4) as well as to each variable’s sub-class (Tables 5, 6) a linguistic value in order to assess the landslide susceptibility. Evaluating the final normalized weights, one conclusion is that, the most significant variables with equal significance contributing to the manifestation of rapid moving masses (rock falls, rock slides), were the lithological units (0.2111) and the slope angle (0.2111) followed by the distance to road network (0.1972) and distance from the tectonic features (0.1833). Limestone formations having considerable percentage of flat-pebble conglomerates were evaluated as the most susceptible formations. Also, areas with slope angle greater than 61° , close to the road network and close to fault zones were ranked as the most susceptible (Table 5). In regard to the slow and very slow movements, the lithological units (0.2375) and distance to road network (0.2000) were the most significant variables followed by the distance from the hydrographic network (0.1844) and the distance from the tectonic features (0.1625). Schist formations and flyschoid sediments were the most susceptible formations according to the calculated normalized weight (Table 6).

Based on the estimated normalized weights, two landslide susceptibility maps were produced in which five categories of susceptibility were introduced (Fig. 11a, b). From the

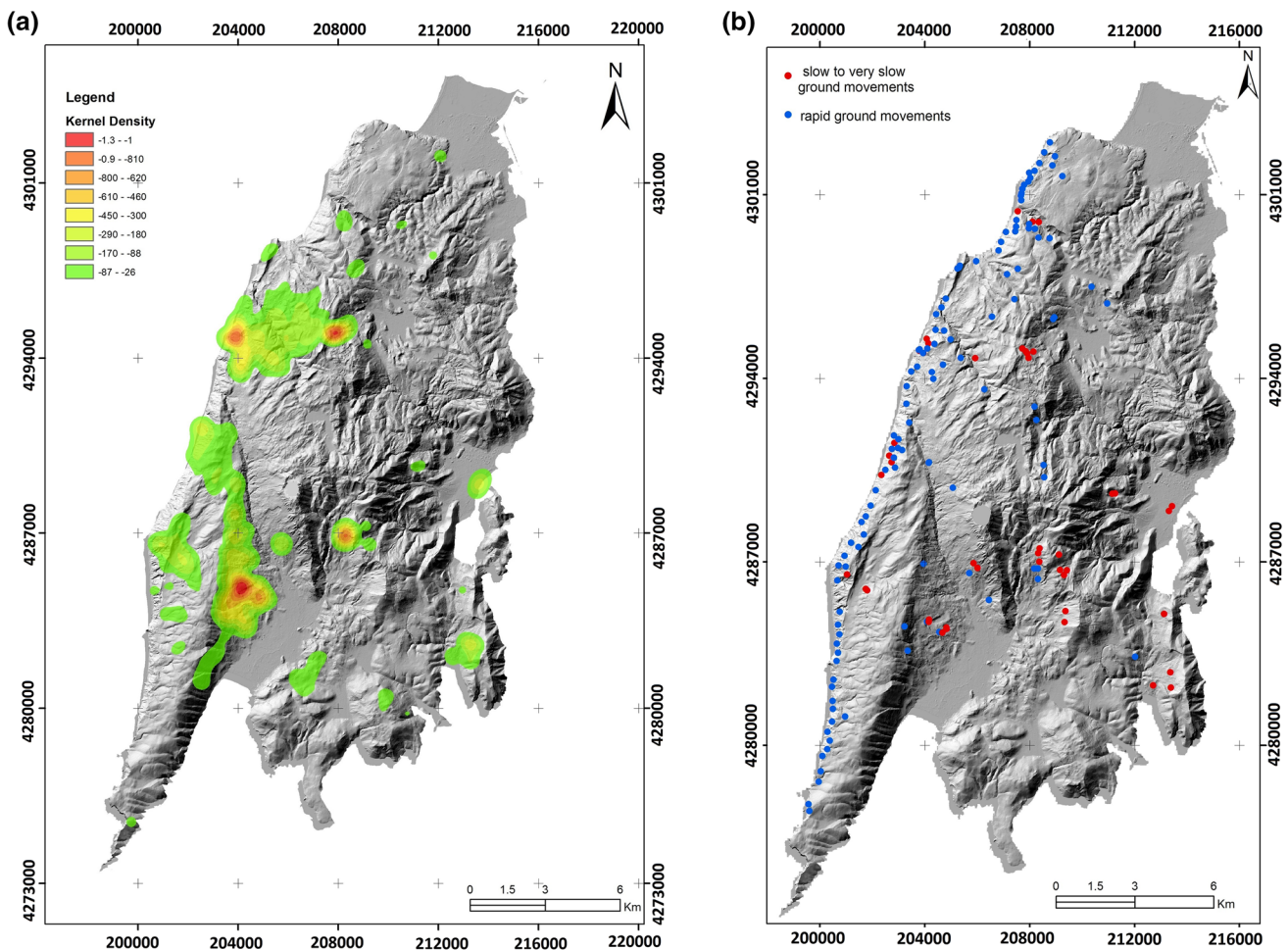


Fig. 10 **a** The kernel density of the final PSI data set including the PSs that presents intensive variability of the displacement rate, with respect to the surrounding points; **b** the landslide inventory map

Table 3 The normalized weights of the landslide-related variables for rapid movements

Thematic layer	A expert (dR = 1.0)	B expert (dR = 1.0)	C expert (dR = 1.0)	Aggregated fuzzy weights	Defuzzified values	Normalized weights
Lithological units	4	5	5	19/3, 27/3, 27/3, 30/3	8.4444	0.2111
Slope angle	5	4	5	19/3, 27/3, 27/3, 30/3	8.4444	0.2111
Slope orientation	3	3	1	6/3, 10/3, 10/3, 17/3	3.6667	0.0917
Distance from tectonic features	4	4	4	5, 7, 7, 10	7.3333	0.1833
Distance from hydrographic network	2	3	3	6/3, 13/3, 13/3, 19/3	4.2222	0.1056
Distance to road network	5	4	4	17/3, 24/3, 24/3, 30/3	7.8889	0.1972

landslide susceptibility map concerning rapid movements, it can be observed that high values of susceptibility were mainly located at the western areas of the island. On the contrary, high values of susceptibility concerning slow to very slow movements cover the entire island and are mainly located within areas covered by soil or soil-like formations,

along the road and river network. Concerning the spatial distribution of the VHS class for slow to very slow movements and with respect to the morphology of the region, almost 88% was estimated to be in areas with slope angle less than 30°. For rapid movements the relevant percentage was about 82% and concerns areas of slope angles lower

Table 4 The normalized weights of the landslide-related variables for slow to very slow movements

Thematic layer	A expert (dR = 1.0)	B expert (dR = 1.0)	C expert (dR = 1.0)	Aggregated fuzzy weights	Defuzzified values	Normal- ized weights
Lithological units	4	5	5	19/3, 27/3, 27/3, 30/3	8.4444	0.2375
Slope angle	3	2	3	6/3, 13/3, 13/3, 19/3	4.2222	0.1188
Slope orientation	2	2	3	3/3, 11/3, 11/3, 17/3	3.4444	0.0969
Distance from tectonic features	3	4	3	11/3, 17/3, 17/3, 24/3	5.7777	0.1625
Distance from hydrographic network	3	4	4	13/3, 19/3, 19/3, 27/3	6.5555	0.1844
Distance to road network	5	3	4	15/3, 22/3, 22/3, 27/3	7.1111	0.2000

than 45° with the majority covered by areas that have slope angles between 30° and 45°.

For the first map, which illustrates the landslide susceptibility concerning rapid movements (Fig. 11a), from a total of 129 failures, 88 (68.21%) were classified into the VHS class, 32 (24.80%) into the HS class and 9 (6.97%) into the MS class, indicating a very good performance. For the second map, which illustrates the landslide susceptibility concerning the slow to very slow movements (Fig. 11b), from a total of 45 failures, 24 (53.34%) were classified into the VHS class, 11 (24.45%) into the HS class and 10 (22.23%) into the MS class. It was also estimated that about 12.83% of the total area was classified as very high susceptibility with regard to slow to very slow movements, while 10.69% of the total area was classified in the highest class of susceptibility with regard to rapid movements (Fig. 12).

Figure 13a, b illustrates the prediction curve rates for the two models after the implementation of the fuzzy logic approach. As it can be seen, for the rapid movements, the AUC values are relatively similar among the experts (0.793, 0.809 and 0.844), indicating a good prediction capability. For the slow to very slow movements the AUC values are also similar (0.734, 0.731, 0.797) indicating, again, a fair to good prediction capability. However, the AUC values that represent the results from the developed methodology are estimated to be much higher, 0.873 and 0.812, respectively. The estimated values indicated that both models had a better prediction capability, in comparison with those produced based on each expert opinion.

Discussion

Several studies support the finding of the present study that remote sensing techniques and field observations are of great assistance for the detection of slow to very slow movements and the construction of an inventory map (Metternicht et al. 2005; Canuti et al. 2007; Parcharidis et al. 2009; Lu et al. 2012). Although PSI data are only valid to identify slow to very slow mass movements, they represent a powerful tool

allowing better understanding of the geometry and kinematics of movements that are not always easy to be identified in the field. The relevant advantage gained from implementation of remote sensing techniques regards the rapid and easily updatable acquisitions of data over wide areas (Canuti et al. 2007). The produced kernel density map assisted the group of experts, in pointing out areas where slow to very slow movements are evident. According to Lu et al. (2012) study, who presented an innovative approach for detecting extremely slow moving landslides based on kernel density estimation, the advantage of the approach is that it takes both PS velocity and spatial distribution of the PSs into consideration.

Based on the results of the fuzzy logic approach followed in the present study and the opinion of experts, the factor lithology played the most significant role in the evolution of rapid and slow to very slow movements. This is in agreement with findings from other studies in which lithology is presented as one of the most important factor controlling ground movements (Koukis and Ziourkas 1991; Koukis et al. 2005; Duman et al. 2006; Henriques et al. 2015). According to Guzzetti et al. (1996) the evolution of landslides are controlled by the relative position of sedimentary formations and tectonic discontinuities, by the relative presence of hard versus weak or soft rocks, and also by the spatial distribution of permeable and impermeable layers. Similarly, Ercanoglou and Temiz (2011) states that lithology dominantly controls the type and mechanism of landslides. In the present study, the contribution of each lithological unit was weighted differently regarding the failure mechanism. The lithological unit that involves carbonate formations was weighted higher regarding their susceptibility to rock falls and low to slides. Although severely fractured carbonate formations can be subjected to rotational or transitional slides presenting a soil-like behavior, field survey data showed that rapid rock falls or debris flows mainly occur within those formations. On the other hand, flyschoid formations were weighted higher regarding their susceptibility to slow to very slow movements and low to rapid movements. As reported by several studies flyschoid formations in the Greek territory

Table 5 Landslide-related variables for rapid movements

Thematic layer	Classes	A expert (dR = 1.0)	B expert (dR = 1.0)	C expert (dR = 1.0)	Aggregated fuzzy weights	Defuzzified values	Nor- malized weights
Lithological units	Recent alluvial deposits (Holocene)	1	2	1	0, 3/3, 3/3, 11/3	1.5555	0.0461
	Recent scree and talus cones	2	1	1	0, 3/3, 3/3, 11/3	1.5555	0.0461
	Flyschoid sediments (blue marls, sandstones sandy clays)	2	3	3	6/3, 13/3, 13/3, 19/3	4.2222	0.1250
	Limestone formations with flat-pebble conglomerates	5	5	5	7, 10, 10, 10	8.3333	0.2467
	Limestone formations	4	4	4	5, 7, 7, 10	7.3333	0.2171
	Dolomite formations	3	4	3	11/3, 17/3, 17/3, 24/3	5.7777	0.1711
	Schist formations	3	3	3	3, 5, 5, 7	5.0000	0.1480
Slope angle	< 15°	1	1	1	0, 0, 0, 3	1.0000	0.0396
	16°–30°	1	3	3	6/3, 10/3, 10/3, 17/3	3.6666	0.1454
	31°–45°	2	3	4	8/3, 15/3, 15/3, 22/3	5.0000	0.1982
	46°–60°	3	4	5	15/3, 22/3, 22/3, 27/3	7.1111	0.2819
	> 61°	5	4	5	19/3, 27/3, 27/3, 30/3	8.4444	0.3348
Slope orientation	0°–45°	4	5	3	15/3, 22/3, 22/3, 27/3	7.1111	0.1370
	45°–90°	3	3	3	3, 5, 5, 7	5.0000	0.0964
	90°–135°	2	1	3	3/3, 8/3, 8/3, 15/3	2.8888	0.0557
	135°–180°	4	3	3	11/3, 17/3, 17/3, 24/3	5.7777	0.1113
	180°–225°	4	5	4	17/3, 24/3, 24/3, 30/3	7.8888	0.1520
	225°–270°	3	3	5	13/3, 20/3, 20/3, 24/3	6.3333	0.1221
	270°–315°	5	4	5	19/3, 27/3, 27/3, 30/3	8.4444	0.1627
Distance from tectonic features	< 100 m	5 (active + overthrust-thrust)	5 (active + overthrust-thrust)	5 (active + overthrust-thrust)	7, 10, 10, 10	9.0000	0.3253
		4 (non-active)	4 (non-active)	5 (non-active)	17/3, 24/3, 24/3, 30/3	7.8888	0.2851
	101–500 m	4 (all)	2 (all)	2 (all)	5/3, 13/3, 13/3, 20/3	4.2222	0.1526
		4 (overthrust-thrust)	3 (overthrust-thrust)	2 (overthrust-thrust)	8/3, 15/3, 15/3, 22/3	5.0000	0.1807
	> 501 m	2	1	1	0, 3/3, 3/3, 11/3	1.5555	0.0562

Table 5 (continued)

Thematic layer	Classes	A expert (dR = 1.0)	B expert (dR = 1.0)	C expert (dR = 1.0)	Aggregated fuzzy weights	Defuzzified values	Nor- malized weights
Distance from hydrographic network	< 50 m	5	5	5	7, 10, 10, 10	9.0000	0.4880
	51–100 m	3	2	4	8/3, 15/3, 15/3, 22/3	5.0000	0.2711
	101–250 m	2	2	3	3/3, 11/3, 11/3, 17/3	3.4444	0.1867
	> 251 m	1	1	1	0, 0, 0, 3	1.0000	0.0542
Distance from road network	Unsurfaced (buffer)						
	< 50 m	5	4	4	17/3, 24/3, 24/3 30/3	7.8888	0.2630
	> 51 m	3	3	2	6/3, 13/3, 13/3, 19/3	4.2222	0.1407
	Surfaced-highway						
	< 50 m	5	5	5	7, 10, 10, 10	9.0000	0.3000
	51–100 m	3	4	4	13/3, 19/3, 19/3, 27/3	6.5555	0.2185
> 101 m	1	1	3	3/3, 5/3, 5/3, 13/3	2.3333	0.0778	

are mainly covered by a thick weathering mantle and are more prone to slides and creep movements (Koukis et al. 2005; Rozos et al. 2008; Sabatakakis et al. 2013).

Based on the produced landslide susceptibility map concerning rapid movements, over 50% of the area classified as very high susceptibility is covered by limestone formations having a slope angle greater than 30°. This is because limestones, in the Ionian and Paxos geotectonic zone, are thick-bedded formations, sometimes fractured with multiple joint systems that, in the western part of the island, form extensive masses of cones of scree materials that can be observed along the base of steep calcareous slopes. Similar to our results, Papathanassiou et al. (2013) reported that the sedimentary rocks covering west- and northwest-facing slopes appear highly fractured with low mechanical properties and in those areas landslide susceptibility is expected to be higher. Concerning slow to very slow movements and based on the analysis of the produced landslide susceptibility map, about 30% of the area classified as very high susceptibility, is covered by Miocene molassic formations, 16% by Upper Triassic limestones and 15% by Miocene marls. The molassic formations and the marls were mostly covered by a thick weathering mantle subjected to sliding or creep movements, especially during periods of prolonged precipitation. This is in agreement with the general observed behavior of these formations in which the weathering process and the decrease in shear strength caused by rainfall is responsible for the manifestation of landslides (Christaras 1997). Respectively, the limestone formations that cover relatively gentle slopes (< 30°), present the same slow movements.

Slope angle was ranked as the second most significant factor, concerning rapid movements. Slopes are formed by

the combined influence of many parameters, such as the intensity of climatic conditions, the weathering processes, the types and density of vegetation, and the discontinuity pattern of geological formations (Huma and Radulescu 1978; Maharaj 1993). Considering that the upper limit of friction angles for silty soils and all other mixed soil formations is 30° and 45°, respectively (Rozos et al. 2008), slow soil failures can be rarely expected along slopes with angles steeper than 45°. On the contrary, rock falls had been observed in the present study with increasing intensity in steeper slopes. Similar to our findings, Papathanassiou et al. (2013) reports that landslide activity is more frequent within areas covered by slope angles higher than 30°, while the highest frequency is observed in areas with slope angle between 40° and 50°.

The distance from road network based on the results of the fuzzy logic approach was ranked as the second most significant factor, concerning slow to very slow movements. This could be justified by the fact that the loss of support at the base of the slopes caused by the construction of road segments, reduces the safety factor, increasing the possibility of landslides. Also, a road segment may affect in very different ways surface runoff, and depending on its location, it may serve as a source of landslides (Pradhan et al. 2010a). From the visual analysis of the produced landslide susceptibility map, it appears that several portions of the road network are highly susceptible, which is in accordance with previous studies highlighting the increased landslide susceptibility near the road network (Papathanassiou et al. 2013; Ganas et al. 2015).

The results of the present study confirmed the initial belief that a group of experts utilizing fuzzy logic approach

Table 6 Landslide-related variables for slow to very slow movements

Thematic layer	Classes	A expert (dR = 1.0)	B expert (dR = 1.0)	C expert (dR = 1.0)	Aggregated fuzzy weights	Defuzzified values	Nor- malized weights
Lithological units	Recent alluvial deposits (Holocene)	1	1	1	0, 0, 0, 3	1.0000	0.0294
	Recent scree and talus cones	2	3	3	6/3, 13/3, 13/3, 19/3	4.2222	0.1242
	Flyschoid sediments (blue marls, sandstones sandy clays)	4	5	4	17/3, 24/3, 24/3 30/3	7.8888	0.2320
	Limestone formations with flat-pebble conglomerates	3	4	3	11/3, 17/3, 17/3, 24/3	5.7777	0.1699
	Limestone formations	3	2	2	3/3, 11/3, 11/3, 17/3	3.4444	0.1013
	Dolomite formations	2	2	2	0, 3, 3, 5	2.6666	0.0784
	Schist formations	5	5	5	7, 10, 10, 10	9.0000	0.2647
Slope angle	< 15°	4	5	2	12/3, 20/3, 20/3, 25/3	6.3333	0.2184
	16°–30°	5	4	4	17/3, 24/3, 24/3 30/3	7.8888	0.2720
	31°–45°	3	3	5	13/3, 20/3, 20/3, 24/3	6.3333	0.2184
	46°–60°	4	2	3	8/3, 15/3, 15/3, 22/3	5.0000	0.1724
	> 61°	3	2	2	3/3, 11/3, 11/3, 17/3	3.4444	0.1188
Slope orientation	0°–45°	4	5	4	17/3, 24/3, 24/3 30/3	7.8888	0.1667
	45°–90°	3	2	1	3/3, 8/3, 8/3, 15/3	2.8888	0.0610
	90°–135°	2	1	1	0, 3/3, 3/3, 11/3	1.5555	0.0329
	135°–180°	4	3	3	11/3, 17/3, 17/3, 24/3	5.7777	0.1221
	180°–225°	5	4	4	17/3, 24/3, 24/3 30/3	7.8888	0.1667
	225°–270°	3	3	5	13/3, 20/3, 20/3, 24/3	6.3333	0.1338
	270°–315°	5	4	5	19/3, 27/3, 27/3 30/3	8.4444	0.1784
315°–0°	4	4	3	13/3, 19/3, 19/3, 27/3	6.5555	0.1385	
Distance from tectonic features	< 100 m	5 (active + overthrust-thrust)	5 (active + overthrust-thrust)	5 (active + overthrust-thrust)	7, 10, 10, 10	9.0000	0.3164
		4 (non-active)	4 (non-active)	5 (non-active)	17/3, 24/3, 24/3 30/3	7.8888	0.2773
	101–500 m	3 (all)	2 (all)	3 (all)	6/3, 13/3, 13/3, 19/3	4.2222	0.1484
		4 (overthrust-thrust)	3 (overthrust-thrust)	3 (overthrust-thrust)	11/3, 17/3, 17/3, 24/3	5.7777	0.2031
	> 501 m	2	1	1	0, 3/3, 3/3, 11/3	1.5555	0.0547

Table 6 (continued)

Thematic layer	Classes	A expert (dR = 1.0)	B expert (dR = 1.0)	C expert (dR = 1.0)	Aggregated fuzzy weights	Defuzzified values	Normalized weights
Distance from hydrographic network	< 50 m	5	5	5	7, 10, 10, 10	9.0000	0.4500
	51–100 m	4	3	4	13/3, 19/3, 19/3, 27/3	6.5555	0.3278
	101–250 m	2	2	3	3/3, 11/3, 11/3, 17/3	3.4444	0.1722
	> 251 m	1	1	1	0, 0, 0, 3	1.0000	0.0500
Distance from road network	Unsurfaced (buffer)						
	< 50 m	5	4	4	17/3, 24/3, 24/3, 30/3	7.8888	0.2817
	> 51 m	2	2	2	0, 3, 3, 5	2.6666	0.0952
	Surfaced-highway						
	< 50 m	5	5	5	7, 10, 10, 10	9.0000	0.3214
	51–100 m	3	3	4	11/3, 17/3, 17/3, 24/3	5.7777	0.2063
	> 101 m	2	2	2	0, 3, 3, 5	2.6666	0.0952

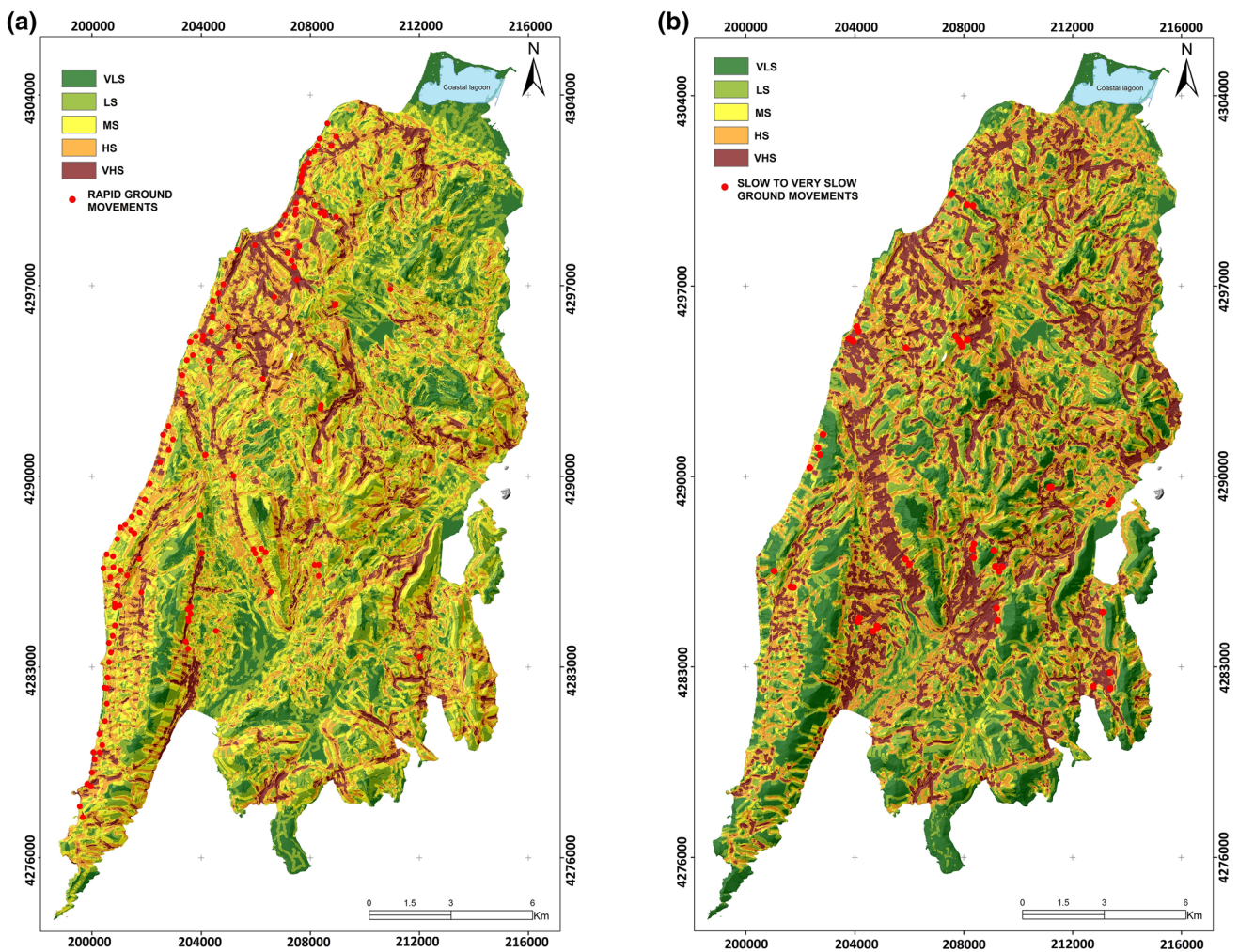


Fig. 11 **a** The landslide susceptibility map of the slow to very slow failures; **b** the landslide susceptibility map of the rapid failures

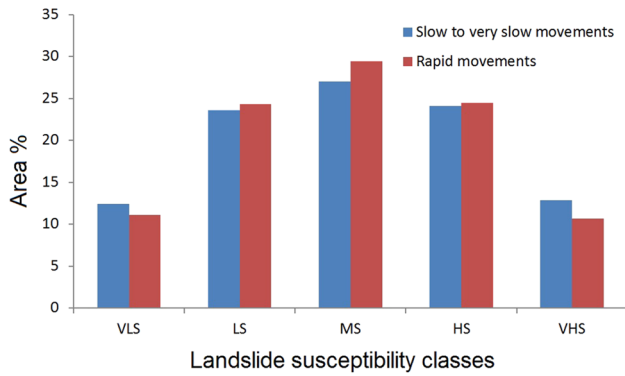


Fig. 12 Percentage of landslide susceptibility classes for both type of movements

can produce a more reliable and accurate landslide susceptibility map. This result is in accordance with previous studies concerning the conclusion that the averaged “judgment” of a group of experts appears to be more accurate than the individual judgment of each expert (Lee and Jones 2004; Chalkias et al. 2016). Moreover, according to Zhu et al. (2014) experts’ knowledge has been accepted to be more reliable, consistent, and generally applicable when the knowledge is formalized under fuzzy logic, as it is in our case. Feizizadeh et al. (2014), highlighted that fuzzy logic approach can be employed to address the presence of vagueness and imprecision of information and also to capture the fuzziness of the experts’ judgment. In both cases of rapid and slow to very slow movements, the prediction capabilities of the developed models are increased with respect to the prediction capability that individually an expert has achieved. The outcomes of the validation procedure confirmed the efficiency of the developed methodology as it presents approximately a 7% increase in the AUC values when the simple fuzzy additive weighting model is utilized.

Conclusions

In the present study, two landslide susceptibility maps concerning the Island of Lefkada, Greece, were produced, providing qualitatively the probable occurrence of two different types of failure: rapid moving failures involving rock falls and rock slides and slow to very slow failures involving earth slides and creep movements. The landslide inventory map for both type of failures, was constructed based on a methodology approach that uses the available landslide records, aerial photos and satellite images, PSI data and fieldwork data. Specifically, the inventory map produced by combining remote sensing techniques and field observations, was of great assistant and proved to be an accurate tool for the detection of slow to very slow movements. Concerning the

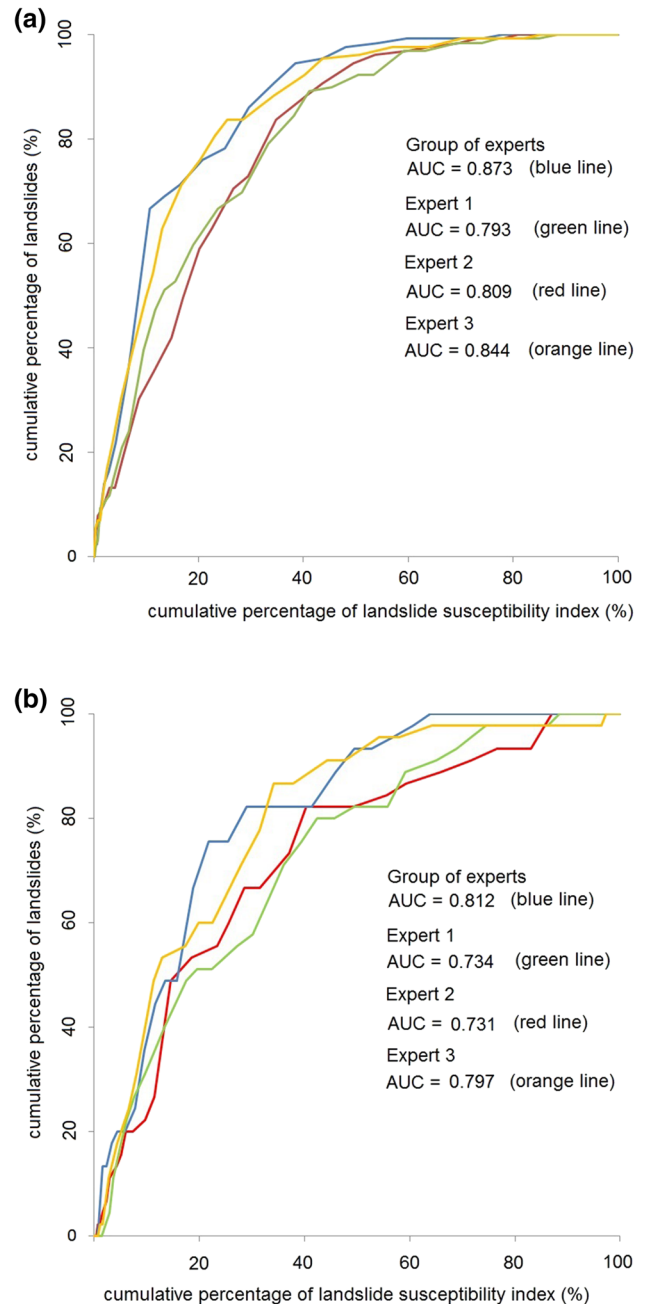


Fig. 13 Prediction rate curves from each expert and overall performance, for **a** rapid ground movements and **b** slow to very slow ground movements

ranking of the variables in accordance with their significance in estimating the landslide susceptibility, the outcomes of the study indicated the following: regarding the rapid moving failures, the most significant variables were lithology and slope angle followed by the distance from road network and from tectonic features. The distance from hydrographic network and slope orientation were identified as the variables with the least significance. Regarding the slow

to very slow movements, lithology and distance from the road network were the most significant variables followed by distance from hydrographic network and from tectonic features. Slope angle and slope orientation were identified as the variables with the least significance with respect to landslide susceptibility. The good prediction capability of the models was confirmed during the validation process. In addition, the initial belief that a group of experts following a fuzzy logic approach could produce a more reliable and accurate landslide susceptibility map, was also confirmed. In both cases, of rapid and slow to very slow movements, the prediction capabilities of the developed models were increased with respect to the prediction capability that each expert had achieved. From the outcomes of the study, it can be concluded that the developed fuzzy logic approach could be efficiently used for landslide susceptibility mapping and for estimation purposes in spatial predictive models.

Acknowledgements The Terrafirma project has funded the SAR imagery processing as well as the geological interpretation presented in this paper. The project is one of the many services supported by the Global Monitoring for Environment and Security (GMES) Service Element Program, promoted and financed by ESA. The project is aimed at providing civil protection agencies, local authorities and disaster management organisms with support in the process of risk assessment and mitigation by using the Persistent Scatterer Interferometry. The authors gratefully acknowledge the Tele-Rilevamento Europa for having processed the SAR data.

References

- Akgün A, Bulut F (2007) GIS-based landslide susceptibility for Arsin–Yomra (Trabzon, North Turkey) region. *Environ Geol* 51:1377–1387
- Aleotti P, Chowdhury R (1999) Landslide hazard assessment: summary review and new perspectives. *Bull Eng Geol Environ* 58(1):21–44
- Alimohammadlou Y, Najafi A, Gokceoglu C (2014) Estimation of rainfall-induced landslides using ANN and fuzzy clustering methods: a case study in Saen Slope, Azerbaijan province. *Iran Catena* 120:149–162
- Ayalew L, Yamagishi H (2005) The application of GIS-based logistic regression for landslide susceptibility mapping in Kakuda-Yahiko Mountains, central Japan. *Geomorphology* 65(1–2):15–31
- Bornovas J (1964) Géologie de l'île de Lefkade. Technical Report, Geological & Geophysics Research, (I.G.S.R.) 10(1), p 142
- Božikov J, Zaletel-Kragelj L (2010) Test validity measures and receiver operating characteristic (ROC) analysis. In: Zaletel-Kragelj L, Božikov J (eds) *Methods and tools in public health, edition: public health in south-eastern Europe: a handbook for teachers, researchers and health professionals*, chapter: test validity measures and receiver operating characteristic (ROC) analysis. Hans Jacobs, Lage, pp 749–770
- Caniani D, Pascale S, Sdao F, Sole A (2008) Neural networks and landslide susceptibility: a case study of the urban area of Potenza. *Nat Hazards* 45:55–72
- Canuti P, Casagli N, Catani F, Falorni G, Farina P (2007) Integration of remote sensing techniques in different stages of landslide response. In: Sassa K, Fukuoka H, Wang F, Wang G (eds) *Progress in landslide science*. Springer, Berlin, pp 251–260
- Carrara A (1983) Multivariate models for landslide hazard evaluation. *J Int Assoc Math Geol* 15(3):403–426
- Carrara A, Cardinali M, Guzzetti F, Reichenbach P (1995) GIS technology in mapping landslide hazard. In: Carrara A, Guzzetti F (eds) *Geographical information systems in assessing natural hazards. Advances in natural technological hazards research*, vol 5. Springer, Dordrecht, pp 135–175
- Casson B, Baratoux D, Delacourt C, Allemand P (2003) “La Clapière” landslide motion observed from aerial differential high resolution DEM. *Eng Geol* 68:123–139
- Castellanos ACJ, Van Westen J (2007) Generation of a landslide risk index map for Cuba using spatial multi-criteria evaluation. *Landslides* 4:311–325
- Chalkias C, Polykretis C, Ferentinou M, Karymbalis E (2016) Integrating expert knowledge with statistical analysis for landslide susceptibility assessment at regional scale. *Geosciences* 6(1):14. <https://doi.org/10.3390/geosciences6010014>
- Champati Ray PK, Dimri S, Lakhera RC, Sati S (2007) Fuzzy-based method for landslide hazard assessment in active seismic zone of Himalaya. *Landslides* 4(2):101–111
- Chou SY, Chang YH, Shen CY (2008) A fuzzy simple additive weighting system under group decision-making for facility location selection with objective/subjective attributes. *Eur J Oper Res* 189(1):132–145
- Christaras B (1997) Landslides in iliolitic and marly formations. Examples from north-western Greece. *Eng Geol* 47:57–69
- Chung CJF, Fabbri AG (2003) Validation of spatial prediction models for landslide hazard mapping. *Nat Hazards* 30(3):451–472
- Cigna F, Bianchini S, Casagli N (2013) How to assess landslide activity and intensity with persistent scatterer interferometry (PSI): the PSI-based matrix approach. *Landslides* 10(3):267–283
- Colesanti C, Wasowski J (2006) Investigating landslides with spaceborne synthetic aperture radar (SAR) interferometry. *Eng Geol* 88(3–4):173–199
- Cruden DM, Varnes DJ (1996) Landslide types and processes. In: *Landslides, investigation and mitigation*. Special report 247. Transportation Research Board, Washington
- Dai FC, Lee CF (2003) A spatiotemporal probabilistic modeling of storm-induced shallow landsliding using aerial photographs and logistic regression. *Earth Surf Process Landf* 28:527–545
- Delacourt C, Allemand P, Berthier E, Raucoules D, Casson B, Grandjean P, Pambrun C, Varel E (2007) Remote-sensing techniques for analysing landslide kinematics: a review. *Bull Soc Geol Fr* 178(2):89–100
- Duman TY, Can T, Gokceoglu C, Nefeslioglu HA, Sonmez H (2006) Application of logistic regression for landslide susceptibility zoning of Cekmece Area, Istanbul. *Turk Environ Geol* 51(2):241–256
- Earthquake Planning and Protection Organization (2000) Greek seismic code (EAK 2000, amended in 2003), Athens (**in Greek**)
- Ercanoglu M, Temiz FA (2011) Application of logistic regression and fuzzy operators to landslide susceptibility assessment in Azdavay (Kastamonu, Turkey). *Environ Earth Sci* 64(4):949–964
- Ercanoglu M, Gokceoglu C (2004) Use of fuzzy relations to produce landslide susceptibility map of a landslide prone area West Black Sea region, Turkey. *Eng Geol* 75(3–4):229–250
- Ermini L, Catani F, Casagli N (2005) Artificial neural networks applied to landslide susceptibility assessment. *Geomorphology* 66(1–4):327–343
- ESRI (2011) ArcGIS Desktop: release 10. Environmental Systems Research Institute, Redlands
- Feizizadeh B, Blaschke T (2013) GIS-multicriteria decision analysis for landslide susceptibility mapping: comparing three methods for the Urmia lake basin, Iran. *Nat Hazards* 65:2105–2128

- Feizizadeh B, Roodposhti MS, Jankowski P, Blaschke T (2014) A GIS-based extended fuzzy multi-criteria evaluation for landslide susceptibility mapping. *Comput Geosci* 73:208–221
- Fell R, Corominas J, Bonnard C, Cascini L, Leroi E, Savage W (2008) Guidelines for landslide susceptibility, hazard and risk zoning for land-use planning. *Eng Geol* 102(1–2):85–98
- Fratini P, Crosta G, Carrara A, Agliardi F (2008) Assessment of rock-fall susceptibility by integrating statistical and physically-based approaches. *Geomorphology* 94(3–4):419–437
- Ganas A, Roumelioti Z, Chousianitis K (2012) Static stress transfer from the May 20, 2012, M 6.1 Emilia-Romagna (northern Italy) earthquake using a co-seismic slip distribution model. *Ann Geophys* 55(4):655–662
- Ganas A, Briole P, Papathanassiou G, Bozionelos G, Avallone A, Melgar D, Argyrakos P, Valkaniotis S, Mendonidis E, Moshou A, Elias P (2015) A preliminary report on the Nov 17, 2015 $M = 6.4$ South Lefkada earthquake, Ionian Sea, Greece, technical report. http://www.earthquakegeology.com/materials/reports/Lefkada_17_Nov_2015-Earthquake_Report.pdf. Accessed 20 Aug 2017
- Gokceoglu C, Aksoy H (1996) Landslide susceptibility mapping of the slopes in the residual soils of the Mengen region (Turkey) by deterministic stability analyses and image processing techniques. *Eng Geol* 44(1–4):147–161
- Gorsevski PV, Jankowski P, Gessler PE (2006) An heuristic approach for mapping landslide hazard by integrating fuzzy logic with analytic hierarchy process. *Control Cybern* 35(1):121–146
- Greif V, Vlcko J (2012) Monitoring of post-failure landslide deformation by the PS-InSAR technique at Lubietova in Central Slovakia. *Environ Earth Sci* 66(6):1585–1595
- Guzzetti F, Cardinali M, Reichenbach P (1996) The Influence of structural setting and lithology on landslide type and pattern. *Environ Eng Geosci* 2(4):531–555
- Guzzetti F, Carrara A, Cardinali M, Reichenbach P (1999) Landslide evaluation: a review of current techniques and their application in a multi-scale study, Central Italy. *Geomorphology* 131:181–216
- Guzzetti F, Reichenbach P, Cardinali M, Galli M, Ardizzone F (2005) Probabilistic landslide hazard assessment at the basin scale. *Geomorphology* 72(1–4):272–299
- Guzzetti F, Mondini A, Cardinali M, Fiorucci F, Santangelo M, Chang KT (2012) Landslide inventory maps: new tools for an old problem. *Earth Sci Rev* 112(1–2):42–66
- Henriques C, Zezere JS, Marques F (2015) The role of the lithological setting on the landslide pattern and distribution. *Eng Geol* 189:17–31
- Hong H, Pradhan B, Xu C, Tien Bui D (2015) Spatial prediction of landslide hazard at the Yihuang area (China) using two-class kernel logistic regression, alternating decision tree and support vector machines. *Catena* 133:266–281
- Huma I, Radulescu D (1978) Automatic production of thematic maps of slope stability. *Bull Int Assoc Eng Geol* 17(1):95–99
- IGME (1963) Geological map of the Lefkada Island (1:50,000). Institute for Geological and Mineral Exploration, Athens
- Ilija I, Tsangaratos P (2016) Applying weight of evidence method and sensitivity analysis to produce a landslide susceptibility map. *Landslides* 13(2):379–397
- Kabassi K (2009) Fuzzy simple additive weighting for evaluating a personalised geographical information system. *New directions in intelligent interactive multimedia systems and services—2 volume 226 of the series studies in computational intelligence*, pp 275–284
- Kaufmann A, Gupta M (1991) Introduction to fuzzy arithmetic: theory and applications. Van Nostrand Reinhold, New York, p 384
- Kokinou E, Papadimitriou E, Karakostas V, Kamperis E, Vallianatos F (2006) The Kefalonia Transform Zone (offshore Western Greece) with special emphasis to its prolongation towards the Ionian Abyssal Plain. *Mar Geophys Res* 27(4):241–252
- Koukis G, Ziourkas C (1991) Slope instability phenomena in Greece: a statistical analysis. *Bull Int Ass Eng Geol* 43(1):47–60
- Koukis G, Sabatakakis N, Nikolaou N, Loupasakis C (2005) Landslides hazard zonation in Greece. In: Proceedings of open symposium on landslides risk analysis and sustainable disaster management by international consortium on landslides, Washington USA, chapter 37, pp 291–296
- Kouli M, Loupasakis C, Soupios P, Vallianatos F (2010) Landslide hazard zonation in high risk areas of Rethymnon Prefecture, Crete Island, Greece. *Nat Hazards* 52(3):599–621
- Kouli M, Loupasakis C, Soupios P, Rozos D, Vallianatos F (2014) Landslide susceptibility mapping by comparing the WLC and WoE multi-criteria methods in the West Crete Island, Greece. *Environ Earth Sci* 72(12):5197–5219
- Lee S (2004) Application of likelihood ratio and logistic regression models to landslide susceptibility mapping using GIS. *Environ Manag* 34(2):223–232
- Lee EM, Jones DKC (2004) Landslide risk assessment. Thomas Telford, London, p 161
- Lee S, Ryu JH, Min K, Won JS (2003) Landslide susceptibility analysis using GIS and artificial neural network. *Earth Surf Process Landf* 28(12):1361–1376
- Lekkas E, Danamos G, Lozios S (2001) Neotectonic structure and neotectonic evolution of Lefkada Island. *Bull Geol Soc Greece* 34(1):157–163
- Li C, Tang H, Ge Y, Hu X, Wang L (2014) Application of back-propagation neural network on bank destruction forecasting for accumulative landslides in the three Gorges Reservoir Region, China. *Stoch Environ Res Risk Assess* 28(6):1465–1477
- Louvari E, Kiratzi A, Papazachos B (1999) The Cephalonia Transform Fault and its extension to western Lefkada Island (Greece). *Tectonophysics* 308(1):223–236
- Lu P, Casagli N, Catani F, Tofani V (2012) Persistent scatterers interferometry hotspot and cluster analysis (PSI-HCA) for detection of extremely slow-moving landslides. *Int J Remote Sens* 33(2):466–489
- Maharaj R (1993) Landslide processes and landslide susceptibility analysis from an upland watershed: a case study from St. Andrew, Jamaica, West Indies. *Eng Geol* 34:53–79
- Marjanovic M, Kovaevic M, Bajat B, Vozemlek V (2011) Landslide susceptibility assessment using SVM machine learning algorithm. *Eng Geol* 123:225–234
- Martha TR, Kerle N, Jetten V, van Westen CJ, Kumar KV (2010) Characterising spectral, spatial and morphometric properties of landslides for semi-automatic detection using object-oriented methods. *Geomorphology* 116:24–36
- Melchiorre C, Matteucci M, Azzoni A, Zanchi A (2008) Artificial neural networks and cluster analysis in landslide susceptibility zonation. *Geomorphology* 94:379–400
- Metternicht G, Hurni L, Gogu R (2005) Remote sensing of landslides: an analysis of the potential contribution to geo-spatial systems for hazard assessment in mountainous environments. *Remote Sens Environ* 98:284–303
- Neaupane KM, Achet SH (2004) Use of back propagation neural network for landslide monitoring: a case study in the higher Himalaya. *Eng Geol* 74(3–4):213–226
- Nefeslioglu HA, Sezer E, Gokceoglu C, Bozkir AS, Duman TY (2010) Assessment of landslide susceptibility by decision trees in the metropolitan area of Istanbul, Turkey. *Math Probl Eng*. <https://doi.org/10.1155/2010/901095> (article ID 901095)
- Neuhauser B, Damm B, Terhorst B (2012) GIS-based assessment of landslide susceptibility on the base of the weights-of-evidence model. *Landslides* 9(4):511–528

- Nikolakopoulos GK (2012) Landslide detection using ALOS optical data. The case of Sykies Village in Andritsena, Greece. In: Proceedings of SPIE—the international society for optical engineering 10/2012. <https://doi.org/10.1117/12.975784>
- Nikolakopoulos GK, Choussiafis C, Karathanassi V (2015) Assessing the quality of DSM from ALOS optical and radar data for automatic drainage extraction. *Earth Sci Inform*. <https://doi.org/10.1007/s12145-014-0199-6>
- Oh HJ, Pradhan B (2011) Application of a neuro-fuzzy model to landslide-susceptibility mapping for shallow landslides in a tropical hilly area. *Comput Geosci* 37(9):1264–1276
- Papadopoulos GA, Karastathis VK, Ganas A, Pavlides SB, Fokaefs A, Orfanogiannaki K (2003) The Lefkada, Ionian Sea (Greece), shock (Mw 6.2) of 14 August 2003: evidence for the characteristic earthquake from seismicity and ground failures. *Earth Planets Space* 55:713–718
- Papathanassiou G, Pavlides S, Ganas A (2005) The 2003 Lefkada earthquake: field observation and preliminary microzonation map based on liquefaction potential index for the town of Lefkada. *Eng Geol* 82:12–31
- Papathanassiou G, Valkaniotis S, Ganas A, Pavlides S (2013) GIS-based statistical analysis of the spatial distribution of earthquake-induced landslides in the island of Lefkada, Ionian Islands, Greece. *Landslides* 10(6):771–783
- Papazachos B, Papazachou C (1989) The earthquakes of Greece. Ziti Publishing, Thessaloniki (in Greek)
- Parcharidis I, Fomelis M, Kourkouli P, Wegmuller U (2009) Persistent scatterers InSAR to detect ground deformation over Rio-Antirio area (Western Greece) for the period 1992–2000. *J Appl Geophys* 68:348–355
- Pham BT, Tien Bui D, Pourghasemi HR, Indra P, Dholakia MB (2015) Landslide susceptibility assessment in the Uttarakhand area (India) using GIS: a comparison study of prediction capability of naive bayes, multilayer perceptron neural networks, and functional trees methods. *Theor Appl Climatol* 122:1–19. <https://doi.org/10.1007/s00704-015-1702-9>
- Pham BT, Tien Bui D, Prakash I, Dholakia MB (2016) Rotation forest fuzzy rule-based classifier ensemble for spatial prediction of landslides using GIS. *Nat Hazards*. <https://doi.org/10.1007/s11069-016-2304-2>
- Pourghasemi HR, Mohammady M, Pradhan B (2012a) Landslide susceptibility mapping using index of entropy and conditional probability models in GIS: Safarood Basin, Iran. *Catena* 97:71–84
- Pourghasemi H, Pradhan B, Gokceoglu C (2012b) Application of fuzzy logic and analytical hierarchy process (AHP) to landslide susceptibility mapping at Haraz watershed, Iran. *Nat Hazards* 63:965–996
- Pourghasemi H, Pradhan B, Gokceoglu C, Moezzi KD (2012c) A comparative assessment of prediction capabilities of Dempster–Shafer and weights-of-evidence models in landslide susceptibility mapping using GIS. *Geomat Nat Hazards Risk* 4:93–118
- Pourghasemi H, Jirandeh AG, Pradhan B, Xu C, Gokceoglu C (2013) Landslide susceptibility mapping using support vector machine and GIS at the Golestan Province. *Iran J Earth Syst Sci* 122(2):349–369
- Pourghasemi H, Moradi H, Fateni Aghda S, Gokceoglu C, Pradhan B (2014) GIS-based landslide susceptibility mapping with probabilistic likelihood ratio and spatial multi-criteria evaluation models (North of Tehran, Iran). *Arab J Geosci* 7:1857–1878
- Pradhan B (2013) A comparative study on the predictive ability of the decision tree, support vector machine and neuro-fuzzy models in landslide susceptibility mapping using GIS. *Comput Geosci* 51:350–365
- Pradhan B, Lee S (2010a) Landslide susceptibility assessment and factor effect analysis: back-propagation artificial neural networks and their comparison with frequency ratio and bivariate logistic regression modeling. *Environ Model Soft* 25(6):747–759
- Pradhan B, Lee S (2010b) Regional landslide susceptibility analysis using back-propagation neural network model at Cameron Highland. *Malays Landslides* 7(1):13–30
- Pradhan B, Akcapinar Sezer E, Gokceoglu C, Buchroithner MF (2010) Landslide susceptibility mapping by neuro-fuzzy approach in a landslide prone area (Cameron Highland, Malaysia). *IEEE Trans Geosci Remote Sens* 48(12):4164–4177. <https://doi.org/10.1109/TGRS.2010.2050328>
- Raspini F, Loupasakis C, Rozos D, Moretti S (2013) Advanced interpretation of land subsidence by validating multi-interferometric SAR data: the case study of the Anthemountas basin (Northern Greece). *Nat Hazards Earth Syst Sci* 1(2):1213–1256
- Raspini F, Loupasakis C, Rozos D, Adam N, Moretti S (2014) Ground subsidence phenomena in the delta municipality region (Northern Greece): geotechnical modelling and validation with persistent scatterer interferometry. *Int J Appl Earth Observ Geoinform* 28:78–89
- Rondoyanni T, Sakellariou M, Baskoutas J, Christodoulou N (2012) Evaluation of active faulting and earthquake secondary effects in Lefkada Island, Ionian Sea, Greece: an overview. *Nat Hazards* 61:843–860
- Rondoyanni-Tsiambaou T (1997) Les seismes et l'environnement géologique de l'île de Lefkade, Grece: Passe. *Eng Geol Environ Balkema*. <https://doi.org/10.1088/1748-9326/7/3/035701>
- Rozos D, Pyrgiotis L, Skias S, Tsagaratos P (2008) An implementation of rock engineering system for ranking the instability potential of natural slopes in Greek territory. An application in Karditsa County. *Landslides* 5(3):261–270
- Rozos D, Barthelos GD, Skillodimou HD (2011) Comparison of the implementation of rock engineering system and analytic hierarchy process methods, upon landslide susceptibility mapping, using GIS: a case study from the Eastern Achaia County of Peloponnesus, Greece. *Environ Earth Sci* 63(1):49–63
- Ruff M, Czurda K (2008) Landslide susceptibility analysis with a heuristic approach in the Eastern Alps (Vorarlberg, Austria). *Geomorphology* 94(3–4):314–324
- Sabatakakis N, Koukis G, Vassiliades E, Lainas S (2013) Landslide susceptibility zonation in Greece. *Nat Hazards* 65(1):523–543
- Sachpazi M, Hirn A, Clement C, Haslinger F, Laigle M, Kissling E, Charvis P, Hello Y, Lepine JC, Sapin M, Ansoerge J (2000) Western Hellenic subduction and Cephalonia Transform: local earthquakes and plate transport and strain. *Tectonophysics* 319:301–319
- Sakkas V, Novali F, Vassilopoulou S, Damiata BN, Fumagalli A (2014) Ground deformation of Zakynthos island (western Greece) observed by PSI and DGPS. *IGARSS 2014, Quebec, Canada*. <https://doi.org/10.13140/2.1.2638.4329>
- Sarkar S, Roy A, Martha T (2013) Landslide susceptibility assessment using information value method in parts of the Darjeeling Himalayas. *J Geol Soc India* 84(4):351–362
- Sezer AE, Pradhan B, Gokceoglu C (2011) Manifestation of an adaptive neuro-fuzzy model on landslide susceptibility mapping: Klang valley, Malaysia. *Expert Syst Appl* 38(7):8208–8219
- Shahabi H, Khezri S, Bin Ahmad B, Hashim M (2014) Landslide susceptibility mapping at central Zab basin, Iran: a comparison between analytical hierarchy process, frequency ratio and logistic regression models. *Catena* 115:55–70
- Tangestani MH (2004) Landslide susceptibility mapping using the fuzzy gamma approach in a GIS, Kakan catchment area, south-west Iran. *Aust J Earth Sci* 51(3):439–450
- Tangestani MH (2009) A comparative study of Dempster–Shafer and fuzzy models for landslide susceptibility mapping using a GIS: an experience from Zagros Mountains, SW Iran. *Asian J Earth Sci* 35(1):66–73

- Tien Bui D, Pradhan B, Lofman O, Revhaug I, Dick OB (2012a) Spatial prediction of landslide hazards in Hoa Binh province (Vietnam): a comparative assessment of the efficacy of evidential belief functions and fuzzy logic models. *Catena* 96:28–40
- Tien Bui D, Pradhan B, Lofman O, Revhaug I (2012b) Landslide susceptibility assessment in Vietnam using support vector machines, decision tree and Naïve Bayes models. *Math Probl Eng* 2012:26. <https://doi.org/10.1155/2012/974638> (article ID 974638)
- Tien Bui D, Pradhan B, Lofman O, Revhaug I, Dick OB (2012c) Landslide susceptibility assessment at Hoa Binh province of Vietnam using an adaptive neuro fuzzy inference system and GIS. *Comput Geosci* 45:199–211
- Tofani V, Raspini F, Catani F, Casagli N (2013) Persistent scatterer interferometry (PSI) technique for landslide characterization and monitoring. *Remote Sens* 5(3):1045–1065
- Torizán J (2016) Elimination of informational redundancy in the weight of evidence method: an application to landslide susceptibility assessment. *Stoch Environ Res Risk Assess* 30(2):635–651
- Tsangaratos P, Benardos A (2014) Estimating landslide susceptibility through an artificial neural network classifier. *Nat Hazards* 74(3):1489–1516
- Tsangaratos P, Iliá I (2016) Landslide susceptibility mapping using a modified decision tree classifier in the Xanthi Prefecture. *Greece Landslides* 13(2):305–320
- Vahidnia MH, Alesheikh AA, Alimohammadi A, Hosseinali F (2010) A GIS-based neuro-fuzzy procedure for integrating knowledge and data in landslide susceptibility mapping. *Comput Geosci* 36(9):1101–1114
- van Westen CJ, Rengers N, Terlien MTJ, Soeters R (1997) Prediction of the occurrence of slope instability phenomena through GIS-based hazard zonation. *Geol Rundsh* 86:404–414
- Varnes DJ IAEG Commission on Landslides and other Mass-Movements (1984) *Landslide hazard zonation: a review of principles and practice*, UNESCO Press, Paris
- Wang W, Xie C, Du X (2009) Landslides susceptibility mapping based on geographical information system, GuiZhou, south-west China. *Environ Geol* 58(1):33–43
- Xu C, Dai F, Xu X, Lee YH (2012) GIS-based support vector machine modeling of earthquake-triggered landslide susceptibility in the Jianjiang River watershed, China. *Geomorphology* 145–146:70–80
- Yalcin A, Reis S, Aydinoglu AC, Yomralioglu T (2011) A GIS-based comparative study of frequency ratio, analytical hierarchy process, bivariate statistics and logistics regression methods for landslide susceptibility mapping in Trabzon, NE Turkey. *Catena* 85:274–287
- Yao X, Tham LG, Dai FC (2008) Landslide susceptibility mapping based on support vector machine: a case study on natural slopes of Hong Kong, China. *Geomorphology* 101:572–582
- Yeon YK, Han JG, Ryu KH (2010) Landslide susceptibility mapping in Injae, Korea, using a decision tree. *Eng Geol* 116(3–4):274–283
- Yilmaz I (2010) Comparison of landslide susceptibility mapping methodologies for Koyulhisar, Turkey: conditional probability, logistic regression, artificial neural networks, and support vector machine. *Environ Earth Sci* 61(4):821–836
- Yin KL, Yan TZ (1988) Statistical prediction models for slope instability of metamorphosed rocks. In: Bonnard C (ed) *Landslides, proceedings of the fifth international symposium on landslides, vol 2*, Balkema, Rotterdam, pp 1269–1272
- Yiping W, Cong C, Gaofeng H, Qiuxia Z (2014) Landslide stability analysis based on random-fuzzy reliability: taking Liangshuijing landslide as a case. *Stoch Environ Res Risk Assess* 28(7):1723–1732
- Youssef AM (2015) Landslide susceptibility delineation in the Ar-Rayth Area, Jizan, Kingdom of Saudi Arabia, by using analytical hierarchy process, frequency ratio, and logistic regression models. *Environ Earth Sci*. <https://doi.org/10.1007/s12665-014-4008-9>
- Youssef AM, Al-Kathery M, Pradhan B (2015a) Landslide susceptibility mapping at AlHasher Area, Jizan (Saudi Arabia) using GIS-based frequency ratio and index of entropy models. *Geosci J* 19(1):113–134
- Youssef AM, Pourghasemi HR, Pourtaghi ZS, Al-Katheeri MM (2015b) Landslide susceptibility mapping using random forest, boosted regression tree, classification and regression tree, and general linear models and comparison of their performance at Wadi Tayyah Basin, Asir Region, Saudi Arabia. *Landslides*. <https://doi.org/10.1007/s10346-015-0614-1>
- Zadeh LA (1965) Fuzzy sets. *Inf Control* 8:338–353
- Zhu AX, Wang R, Qiao J, Qin CZ, Chen Y, Liu J, Du F, Lin Y, Zhu T (2014) An expert knowledge-based approach to landslide susceptibility mapping using GIS and fuzzy logic. *Geomorphology* 214:128–138
- Zimmermann HJ (2001) *Fuzzy set theory—and applications*, 4th rev. ed. Kluwer Academic Publishers, Boston